PRODUCTION OF DENSE COMPACT BILLET FROM Ti-ALLOY POWDER USING EQUAL CHANNEL ANGULAR EXTRUSION

Final Report
4/06/2007

Rimma Lapovok and Dacian Tomus

ARC Centre of Excellence for Design in Light Metals

Dept. of Materials Engineering, Monash University

Clayton, Melbourne, VIC 3800, Australia

Report Documentation Page

Form Approved
OMB No. 0704-0188

1. REPORT DATE	2. REPORT TYPE	3. DATES COVERED
09 AUG 2007	**FInal**	**03-10-2005 to 03-08-2007**

4. TITLE AND SUBTITLE
Production of fully dense compact billet from Ti-alloy powder

5a. CONTRACT NUMBER
FA520905C0034

5b. GRANT NUMBER

5c. PROGRAM ELEMENT NUMBER

6. AUTHOR(S)
Rimma Lapovok

5d. PROJECT NUMBER

5e. TASK NUMBER

5f. WORK UNIT NUMBER

7. PERFORMING ORGANIZATION NAME(S) AND ADDRESS(ES)
Monash University,School of Physics and Materials Engineering,Clayton Victoria 3168,Australia,AU,3168

8. PERFORMING ORGANIZATION REPORT NUMBER
N/A

9. SPONSORING/MONITORING AGENCY NAME(S) AND ADDRESS(ES)
AOARD, UNIT 45002, APO, AP, 96337-5002

10. SPONSOR/MONITOR'S ACRONYM(S)
AOARD

11. SPONSOR/MONITOR'S REPORT NUMBER(S)
AOARD-054031

12. DISTRIBUTION/AVAILABILITY STATEMENT
Approved for public release; distribution unlimited

13. SUPPLEMENTARY NOTES

14. ABSTRACT

ABSTRACT The project was aimed at an investigation of the potential for cost-effective, efficient consolidation of pre-alloyed (PA) Ti-6Al-4V (HDH) powder at temperatures of 400?C and below using Equal Channel Angular Extrusion (ECAE), with applied back pressure. The limit on processing temperature was imposed to minimize the contamination of powder and compact with gaseous constituents known to be harmful to resultant properties. An analysis of existing published investigations of current processing techniques, most notably those involving hot isostatic pressing (HIP), reveals that relative densities of 98-100% can only be obtained at processing temperatures in excess of 800?C. For such methods, and temperatures below 400?C, the relative densities achievable are typically of the order of 77%, when starting with an initial ?tape? density of 63%. In this context, the project goals, of reducing the processing temperature of PA powder compaction below 400?C while achieving a relative density above 98%, are to be seen as quite challenging. The novelty of the approach arises from the notion that severe shear deformation could prove an important factor for improving consolidation at relatively low processing temperatures. It has been shown that the use of ECAE with back pressure at 400?C permits production of compacts with relative densities in the range 98.3-98.6% and green strengths up to 750 MPa. The improvements in density and green strength are attributed to enhancement of self-diffusion rates at low temperatures that are in turn the result of an excess of structural defects created during severe shear deformation and the effects of imposed hydrostatic pressure (back pressure). It has also been shown that further increases in relative density (to in excess of 99%) may potentially be obtained by increasing the component of hydrostatic pressure or by manipulation of powder/compact microstructure to increase of the volume fraction of the β phase constituent and the ratio of β:α phase in the microstructure. A modest increase in the β ? phase fraction from 5.5% (as-received condition) to 10% (after heat treatment) has been shown to contribute to a measurable increase in relative density from 98.3% to 98.9% at a processing temperature of 400?C and a back pressure of 350MPa.

15. SUBJECT TERMS

16. SECURITY CLASSIFICATION OF:			17. LIMITATION OF ABSTRACT	18. NUMBER OF PAGES	19a. NAME OF RESPONSIBLE PERSON
a. REPORT	b. ABSTRACT	c. THIS PAGE			
unclassified	**unclassified**	**unclassified**	**Same as Report (SAR)**	**48**	

EXECUTIVE SUMMARY

The project was aimed at an investigation of the potential for cost-effective, efficient consolidation of pre-alloyed (PA) Ti-6Al-4V (HDH) powder at temperatures of 400ºC and below using Equal Channel Angular Extrusion (ECAE), with applied back pressure. The limit on processing temperature was imposed to minimise the contamination of powder and compact with gaseous constituents known to be harmful to resultant properties.

An analysis of existing published investigations of current processing techniques, most notably those involving hot isostatic pressing (HIP), reveals that relative densities of 98-100% can only be obtained at processing temperatures in excess of 800ºC. For such methods, and temperatures below 400ºC, the relative densities achievable are typically of the order of 77%, when starting with an initial 'tape' density of 63%. In this context, the project goals, of reducing the processing temperature of PA powder compaction below 400ºC while achieving a relative density above 98%, are to be seen as quite challenging.

The novelty of the approach arises from the notion that severe shear deformation could prove an important factor for improving consolidation at relatively low processing temperatures. It has been shown that the use of ECAE with back pressure at 400ºC permits production of compacts with relative densities in the range 98.3-98.6% and green strengths up to 750 MPa. The improvements in density and green strength are attributed to enhancement of self-diffusion rates at low temperatures that are in turn the result of an excess of structural defects created during severe shear deformation and the effects of imposed hydrostatic pressure (back pressure).

It has also been shown that further increases in relative density (to in excess of 99%) may potentially be obtained by increasing the component of hydrostatic pressure or by manipulation of powder/compact microstructure to increase of the volume fraction of the β phase constituent and the ratio of β:α phase in the microstructure. A modest increase in the β – phase fraction from 5.5% (as-received condition) to 10% (after heat treatment) has been shown to contribute to a measurable increase in relative density from 98.3% to 98.9% at a processing temperature of 400ºC and a back pressure of 350MPa.

CONTENTS

1. INTRODUCTION

The production of wrought Ti-alloys is an energy consuming process. The standard Ti alloy VAR melting practice requires re-melting of the initial ingot two/three times [1]. The high cost of processing of Ti billets limits the possible wider application of Ti-alloys despite their unique combination of mechanical properties. The alternative P/M processes were developed with much lower energy requirements. The cost saving on parts produced by P/M methods is estimated to be 20-50% compared to forged parts, [2]. Of two different approaches using either blended elemental or pre-alloyed powders, the Blended Elemental (BE) method, in which Ti powder is blended with alloying elements added as elemental or master alloy powder, is the less expensive [3]. The method using Pre-Alloyed (PA) powders produces more expensive compacts from the pre-alloyed stock, but it has the advantage of producing a higher level of mechanical properties in the product and more uniform product chemistry, as individual particles have the same chemical composition.

The powder blend is consolidated at room temperature under pressures of up to 410 MPa to produce a “green” compact with 85-90% theoretical density. Two methods of compaction,-cold pressing (CP) and cold isostatic pressing (CIP)- are used for compaction. In CP, a mechanical or hydraulic press is used to press blended powder into the die. The variation in density along the thickness, and the inability of powder to flow under hydrostatic pressure at room temperature, limit the achievable product to simple shapes [3]. In CIP, the powder is encapsulated in relatively expensive soft cans and hydrostatic pressure is applied to the external surfaces of this soft tooling, increasing the processing cost. Both methods of compaction are followed by a sintering operation in a vacuum furnace at a temperature higher than 1200°C to homogenize the part and to improve its density.

Among the various compaction processes, hot isostatic pressing (HIP) is normally used for consolidating PA powder. The typical scheme is that a container filled with PA particles is hermetically sealed after an evacuation cycle and is then subjected to a hydrostatic pressure at high temperature in a pressure vessel. Sintering resulting from HIP depends on the packing density of the powder, which depends in turn on the shape and size distribution of the particles [3].

However, the presence of pores after the sintering is observed and reported in several publications such as, for example, in [4,5], Fig. 1. The presence of porosity after sintering is a common problem in both the BE and the PA methods, and it influences significantly the quality and mechanical properties of the compact. Development of a new method for compaction, with the potential for significantly reducing the level of porosity, would, therefore, be beneficial.

The expense of the HIP process also makes alternative methods of consolidation attractive. Pre-alloyed powders do not have the compositional inhomogeneity associated with blended elemental powders and so do not require the same high temperatures used in sintering of BE powders to accelerate the diffusion of alloying elements. For TI-6Al-4V powder, HIP is typically performed at temperature of 845-955°C and a pressure of about 105 MPa for 2-4 hours. Colder HIP cycles have produced compacts with low mechanical properties (no green strength) due

apparently to the spherical or equiaxed shape of the particles. Therefore, the development of compaction methods viable for performing warm compaction at significantly lower temperatures with increased bond between particles would again be beneficial.

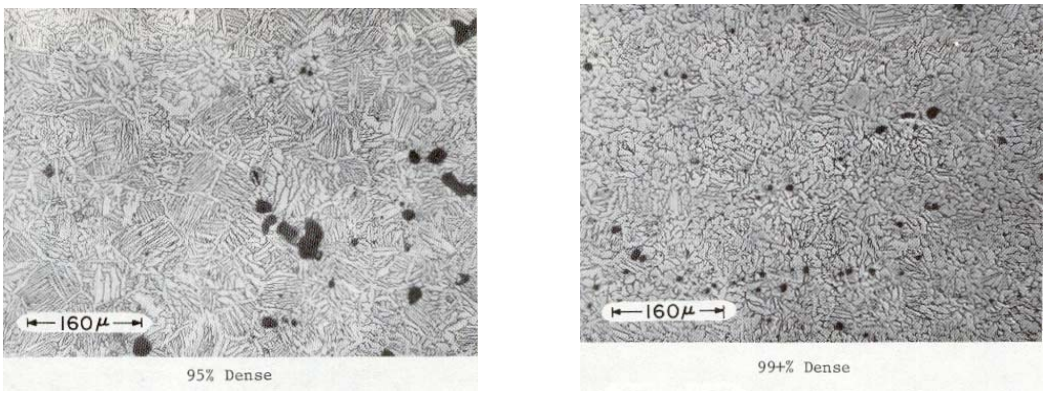

Fig. 1 Typical microstructures of Ti-6Al-4V in the as-sintered conditions. From ref. [5]

2. AIMS

This present research was aimed at enhanced compaction of Ti-6Al-4V PA powder at lower temperatures (below 400ºC) with simultaneous elimination of porosity using Equal Channel Angular Extrusion (ECAE) with back-pressure. It was anticipated that this approach would lead to potentailly decreasing the manufacturing cost by exclusion of the evacuation stage, elimination of the use of soft cans, and removal of the sintering stage for the forging stock. It would also potentially reduce to a minimum the gaseous contamination by decreasing the temperature of compaction.

3. LITERATURE REVIEW

The potential for producing Ti-6Al-4V billet from different BE powders by cold pressing and sintering of the green compact has been investigated in [6,7,8]. The mixtures were made either from elemental powders (Ti, Al, V) – designated EP or from powders of master alloys (65Ti-35Al, 25Al-75V) – designated MAP. The relative densities of the green and sintered compacts, produced by cold pressing and sintering at 1360ºC, are shown in Fig. 2., as a function of cold compaction pressure.

Assuming that MAP powder represents the closest to the PA powder case, it can be noticed that to obtain maximum densities, of about **87%** in green compact and about **97.5%** in sintered compact, the pressures required are extremely high (at the level of 1000 MPa).

There remain some reservations concerning the use of BE powders for production of Ti-6Al-4V compacts by a combination of cold pressing followed by sintering. Such reservations arise from the observation [8] that sintering can decrease the relative

density due to the low meltng temperature of aluminium. Analysis of other published works on production of Ti-6Al-4V compacts by PM routes [9,10,11] shows that HIP of PA powder is still the best in terms of quality, although it is not a cost-effective method of manufacturing compacts.

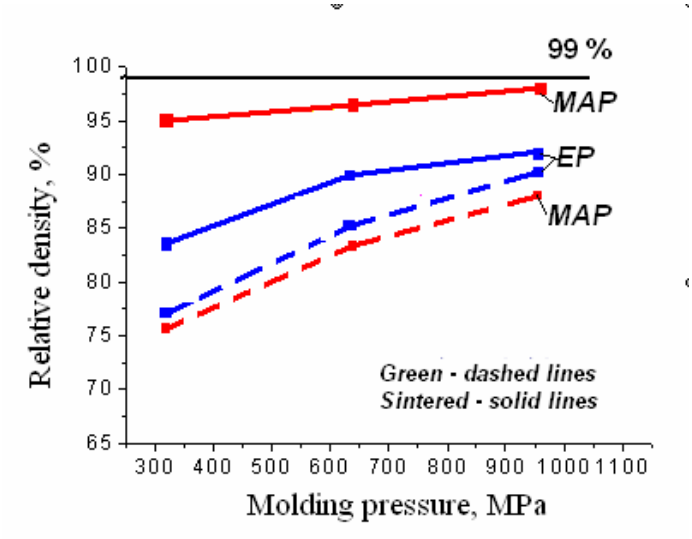

Fig. 2 From ref. [7]. Relative densities of Ti-6Al-4V green and sintered compacts from two BE powders versus pressure of compaction.

The effects of HIP processing conditions on the resulting relative density of compacts produced from PREP Ti-6Al-4V powder are reported in [12]. The authors investigated different HIP parameters, where temperature ranged between 20 and 850ºC, pressures between 10 and 60 MPa, and compaction times between 0 and 60 min. As can be seen from Fig. 3, relative densities in the range 98-100% were obtained at temperatures higher than 800ºC, while at temperatures lower than 400ºC the relative density was below 77%, when starting from an initial 'tape' density of 63%.

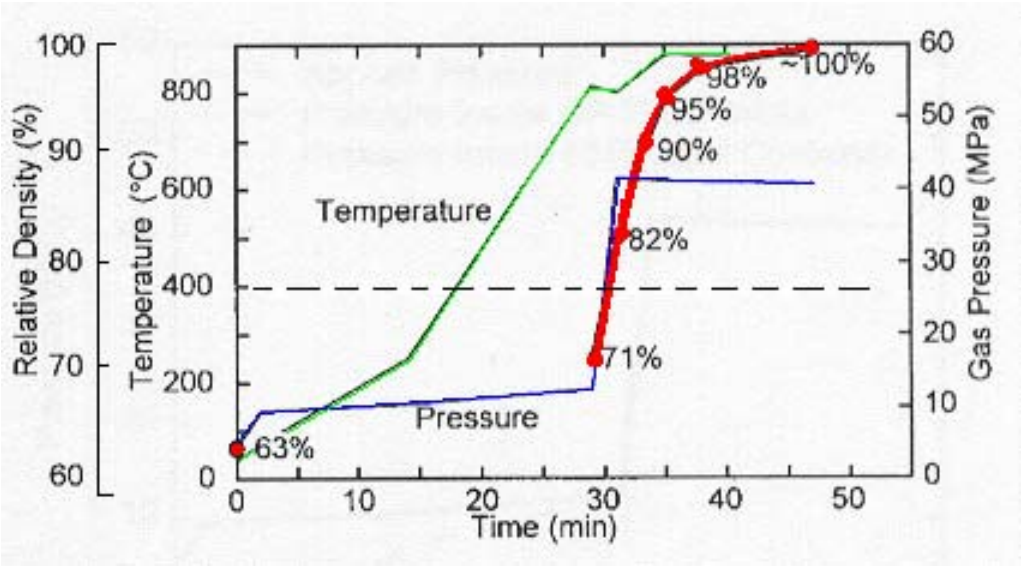

Fig. 3 From ref. [12]. HIP processing conditions and resulting relative densities for PREP Ti-6Al-4V powder

In this context, the aim of this current project, which was to reduce the temperature of PA powder compaction to below 400ºC can be seen to be quite challenging. The method of compaction suggested was the process of Equal Channel Angular Extrusion (ECAE) with Back-Pressure.

ECAE is a well-known process for production of bulk ultrafine-grained (or nanostructured) materials with unique mechanical and physical properties [13]. It has also been shown that superimposed hydrostatic pressure in ECAE, sustained by back pressure, plays an important role in processing of bulk nanomaterials, Fig. 4 [14]. However, despite the extensive publications on the potential of ECAE processing, few publications have touched upon the application of ECAE to compaction of powder [15, 16,17]. It has been found that ECAE with back pressure enhances compaction very effectively and decreases the level of residual porosity, due to the combination of simple shear with superimposed hydrostatic pressure [14].

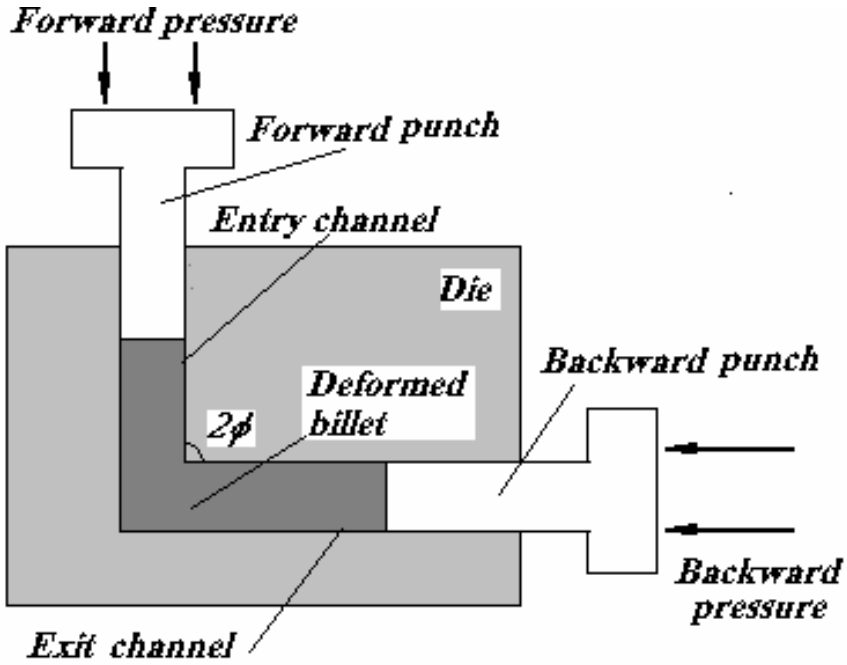

Fig. 4 Schematic of Equal Channel Angular Extrusion with Back-Pressure

4 MATERIAL CHARACTERIZATION AND EXPERIMENTAL TECHNIQUES

4.1 Material Characterization

The research utilised a hydride-dehydride (HDH), pre-alloyed Ti-6Al-4V powder supplied by Phelly Materials (U.S.A.) Inc., with a chemical composition as shown in Table 1.

Table 1. Chemical composition of the powder (wt%)

Element	**Al**	**V**	**O**	**Fe**	**C**	**H**	**N**	**Cu**	**Sn**	**Ti**
ASTM F1580-01	5.5~6.75	3.5~4.5	0.2	0.3	0.08	0.015	0.05	0.1	0.1	Balance
Testing results	6.24	4.19	0.19	0.09	0.03	0.009	0.04	<0.05	<0.05	Balance

Scanning electron microscopy (SEM) of unmounted powder revealed an irregular shape and rough surfaces for individual particles within the range 50-150 μm, which confirmed the sieve analysis of the particle size provided by the manufacturer. The SEM images of unmounted powder are shown in Fig. 5a. The optical micrographs of Fig. 5b show the existence of cracks in larger particles due to comminution of brittle hydride as part of the HDH powder processing method.

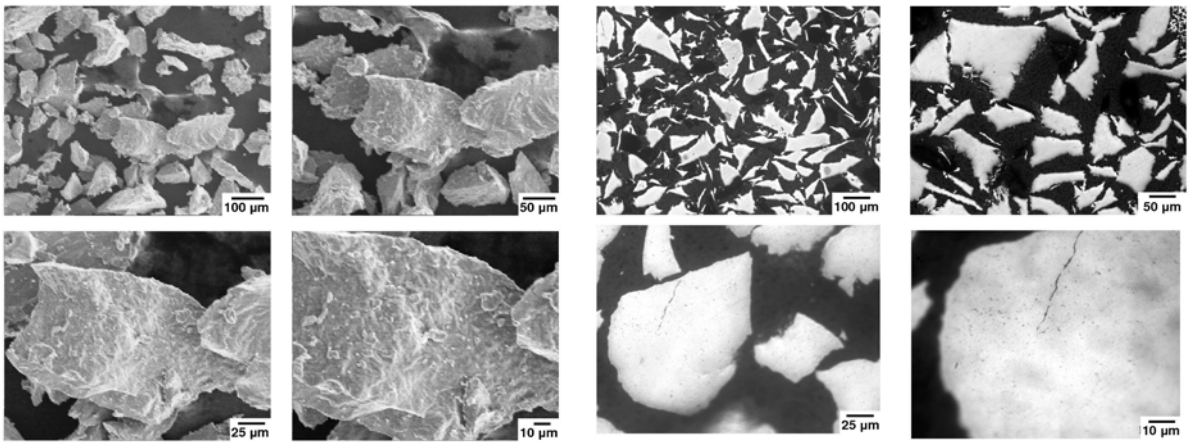

(a) (b)

Fig. 5 Images of as-received Ti6Al4V powder
(a) Scanning Electron Micrographs; (b) Optical Micrographs.

The Vickers microindentation hardness of individual particles of Ti-6Al-4V powder mounted in epoxy had a value of 358 HV, based on an average of 20 measurements with a standard deviation of 1.56. X-ray diffraction (XRD) analysis, Fig. 6, carried out to determine the constituent phases of Ti-6Al-4V powder revealed predominantly α-phase, with ß-phase being below 5%.

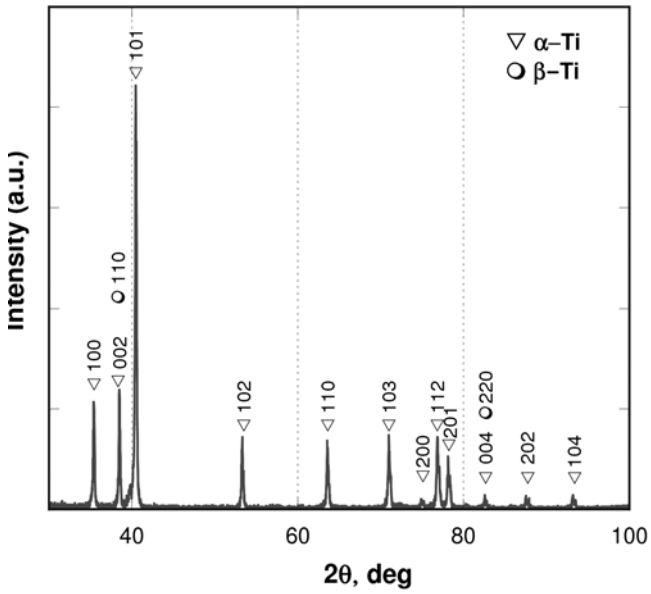

Fig. 6 XRD analysis of Ti6Al4V powder showing peaks of α and ß-Ti.

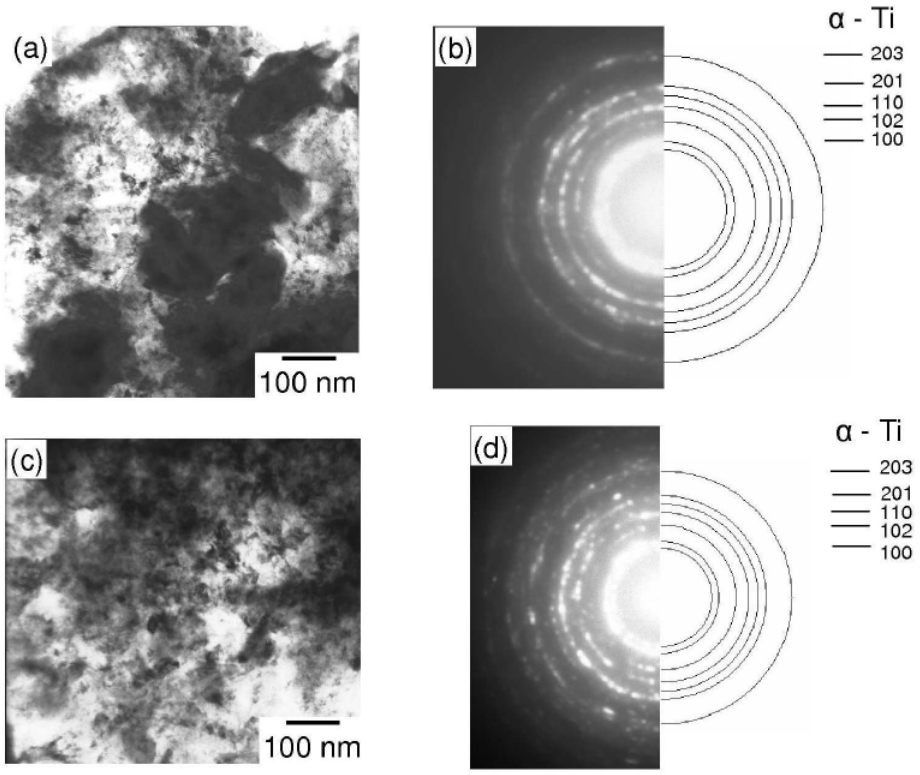

Fig. 7 TEM micrographs of as-received Ti-6Al-4V powder, after subjecting to additional mechanical grinding
(a) and (c) bright field images, (b) and (d) corresponding selected area electron diffraction patterns.

That phase-ratio was also confirmed by transmission electron microscopy (TEM) observation. The particle size of as-received powder was unsuitable for TEM observation and it was for this reason that additional grinding was performed on as-received powder The TEM micrographs are shown in Fig.7. Very fine particles can be observed in the bright field images in Figs.7a and 7c. Figs. 7b and 7d show the corresponding diffraction patterns indexed as the α-Ti phase. The discontinuous rings are evidence of a small crystallite size in the range of nanometers, probably due to the deformation during grinding. The TEM observation revealing predominantly α -Ti phase is in agreement with XRD analysis.

Other constituents or contaminants like titanium oxides or hydrides were below detectable limits.

Differential Scanning Calorimetry was carried out on the as-received powder in the temperature range between room temperature and 500°C, primarily to assess the potential presence of hydrogen The presence of hydrogen in Ti alloys can potentially be detected by DSC analysis, through the observation of various peaks attributable to different endothermic reactions associated with dehydrogenation [18]. However, instead of multiple peaks, the DSC curve in Fig. 8, obtained by heating the as-received Ti-6Al-4V powder at a constant heating rate of 20°C/min, shows a smooth linear increase with no evidence of a dehydrogenation reaction. Equally there is no evidence of any other phase transformations occurring over the range of room temperature up to 450°C.

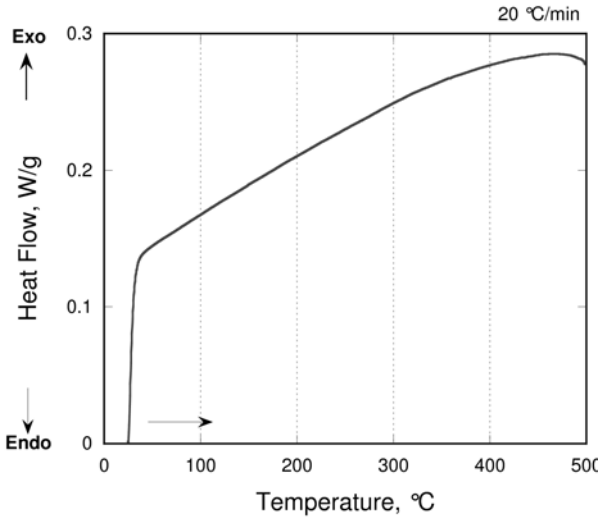

Fig. 8 DSC analysis of as-received Ti6Al4V powder.

4.2 Experimental Techniques

ECAE with back pressure was performed using a specially designed unit, Fig. 9, with a die located in the shrink collar, incorporating heating elements, which provide capability for conducting isothermal ECAE within the temperature range between 20 and 450°C. The back-pressure is regulated by horizontal hydraulic cylinder, equipped with a bleed valve to maintain the pressure at a preset level between 20 and 500 MPa. The unit is placed in a 1000kN press which exercises the forward pressure of extrusion.

Fig. 9 Unit for elevated-temperature ECAE with back-pressure at Monash University

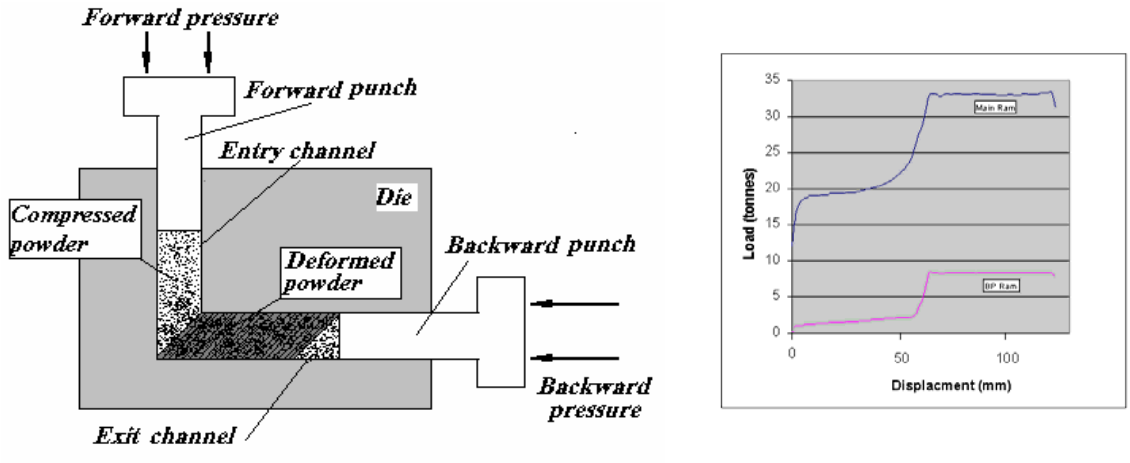

(a) (b)

Fig. 10 The schematic of powder compaction (a) and graphs of forward and backward forces during compaction (b)

The vertical entry channel is 75 mm in length and makes a 90°angle with the horizontal exit channel. The powder was poured directly into the vertical entry channel and during pouring the back-pressure punch was positioned deep within the exit channel to contain powder within the vertical channel. As forward pressure is gradually increased, a large hydrostatic pressure is created in the vertical channel, pre-compacting the powder. When the pressure exceeds the pre-set backward pressure, shear plastic deformation of the pre-compact commences and it flows into the exit channel against the back pressure punch, Fig. 10.

The green strength of the compacts was measured according to ASTM B 312 -96 using a three-point bend test as shown in Fig 11. Green strength is defined as the stress required to fracture a specimen, and is calculated using Equation 1. The rig and test specimen were scaled down by a 1/3 ratio, with the dimensions of the specimen equal to 10.5 x 4.2 x 2.1 mm, and the span being 8.6mm.

$$S = \frac{3PL}{2t^2 w} \tag{1}$$

where S - green strength (MPa); P - force required to rupture (N); L - length between support (mm); w - width of specimen (mm); and t - thickness of specimen (mm). The samples were cut parallel to the extrusion direction.

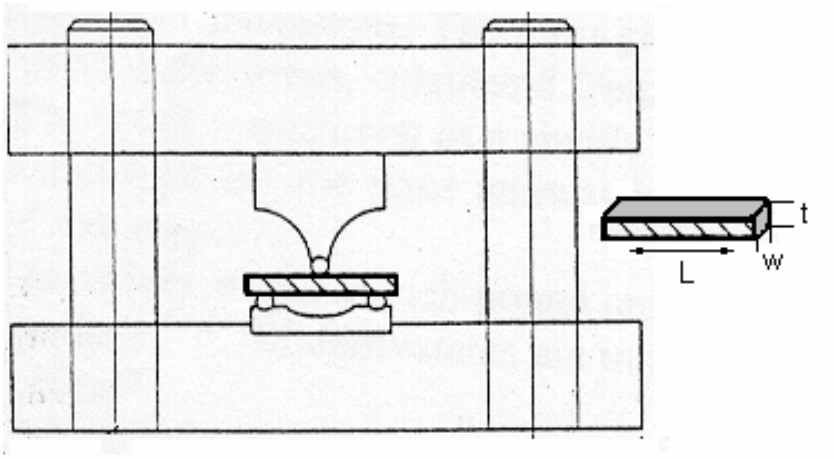

Fig. 11 Schematic of green strength test

The quality of the compact produced by ECAE was evaluated by Vickers Hardness and density measurements. The Vickers Hardness under a 1kg load with indent time of 10 s was calculated from ten individual measurements. The density of compacts was defined by Archimedes' method (ASTM, B311-93) using tetrachlorethylene, with a density of 1.62g/cm^3, as the immersion liquid. The theoretical density of Ti-6Al-4V alloy is 4.45 g/cm^3.

The size distribution of pores and the ratio of alpha to beta phases were measured by computer-assisted imaging analysis of images obtained by light and scanning electron microscopy (SEM), respectively. The powder morphology, deformation mechanisms and microstructural evolution were analysed using SEM (JEOL JSM-6300F at 15kV) and transmission electron microscopy (TEM; Philips CM20 at 200 kV). Metallographic sample preparation consisted of grinding on SiC paper, polishing with diamond, and etching with Kroll's reagent (5% nitric acid, 10% HF, 85% water). TEM samples in the form of 3mm diameter discs were cut from the compact and electropolished in a twin-jet TENUPOL 5 operating at -50°C using a solution of 5wt% perchloric acid in 95wt% methanol. The average coherent lattice domain size and the lattice strain were calculated from XRD results obtained using a Philips diffractometer equipped with a Cu anode at 40kV and 25 mA.

The heat treatment of the as-received powder was performed by encapsulating the powder in a quartz tube and heating to 730, 850 and 1065°C, followed by furnace and air cooling.

5. EXPERIMENTS

A comprehensive summary of the individual experiments carried out is presented in Table 2.

Table 2 Conditions under which ECAE experiments were conducted

N	BP, MPa	Temp,ºC	Relative density, %	Comments
1	43	RT	95.3	dry lubricant
2	175	RT	95.3	dry lubricant
3	262	RT	95.6	dry lubricant
4	21	100	95.4	dry lubricant
5	43	100	96	dry lubricant
6	175	100	96.2	dry lubricant
7	262	100	96.4	dry lubricant
8	21	200	95.5	dry lubricant
9	43	200	96.5	dry lubricant
10	175	200	96.5	dry lubricant
11	262	200	97	dry lubricant
12	21	300	95.7	dry lubricant
13	43	300	96.8	dry lubricant
14	175	300	97.1	dry lubricant
15	262	300	97.2	dry lubricant
16	21	400	97.4	dry lubricant
17	43	400	97.5	dry lubricant
18	175	400	**98.2**	dry lubricant
19	305	400	**98.1**	dry lubricant
20	305	400	**98.0**	dry lubricant
21	350	400	**98.3**	dry lubricant
21	262	400	**98.2**	dry lubricant
22	262	400	98	wet lubricant
23	305	400	98.1	wet lubricant
24	350	400	97.3	wet lubricant
25	436	400	97.4	wet lubricant
26	524	400	97.8	wet lubricant
27	436	400	97.1	wet lubricant
28	524	400	97.7	wet lubricant
29	350	400	97.4	Al tubes
30	393	400	97.8	Al tubes
31	350	400	97.9	Al- tube
32	436	400	97.6	Al tubes
33	480	400	**98.6**	Al tubes
34	524	400	95.8	closed die compression
35	524	400	96.4	closed die compression
36	305	400	97.9	closed die compression
37	262	400	97.7/98.2	1 ECAP pass / 2 ECAP pass
38	262	400	97.8/98.3	1 ECAP pass / 2 ECAP pass
39	262	400	97.9/98.3	1 ECAP pass / 2 ECAP pass
40	262	400	97.9	hold 1 hour under pressure
41	262	400	97.8	hold 1 hour under pressure

42	262	400	97.8/98.2	before/after sintering
43	305	400	97.9/98.7	before/after sintering
44	350	400	**98.7**	4h@730ºC, furnace cooled
45	350	400	**98.8**	4h@850ºC, furnace cooled
46	350	400	**98.9**	4h@1065ºC,furnace cooled
47	350	400	97.3	4h@730ºC, air cool., closed die compr.
48	436	400	97.4	4h@730ºC, air cool., closed die compr.
49	524	400	97.3	4h@730ºC, air cool., closed die compr.

*BP - Back Pressure.

6. EXPERIMENTAL RESULTS

6.1 ECAE Compaction of Ti-6Al-4V Powder at Room Temperature

The feasibility of ECAE compaction of powder at room temperature was assessed by performing ECAE at three different levels of back pressure. At the minimum back-pressure, created by friction force alone, densification of powder in the vertical channel was achieved by direct compression, but the compact was destroyed in the exit channel by subsequent shear deformation, Fig. 12.

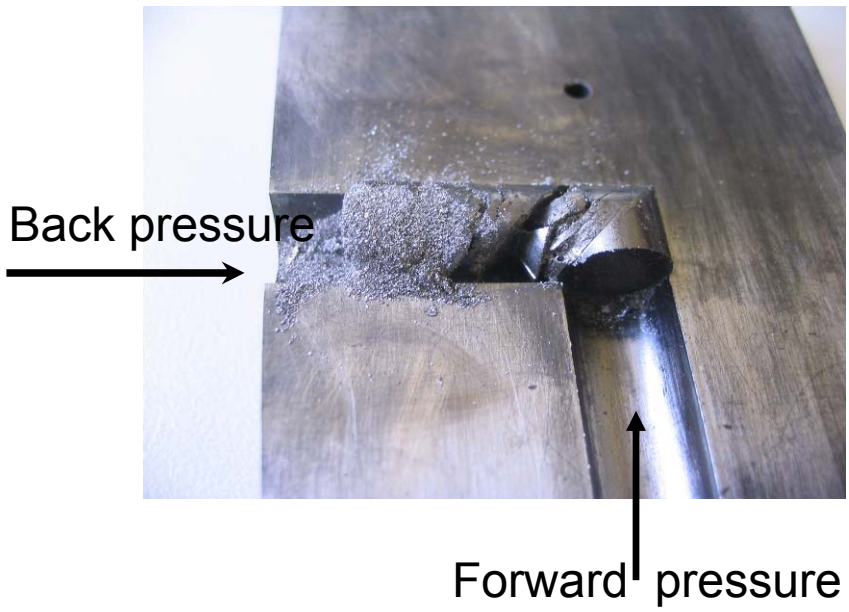

Fig. 12 ECAE of the powder at ambient temperature with minimum back-pressure

Any increase of back-pressure led to improved pre-compaction in the vertical channel to an initial density of 89-91%, Fig. 13a, and permitted ECAE, which improved the density typically to values of 95.3-95.6%. However, some cracks were present after processing, Fig. 13b, presumably due to the limited ductility of Ti-6Al-4V at room temperature. Cracks occurred at the surface of the billet in contact with the inner surface of the die, which is typical for ECAE processing conducted in the absence of

back pressure [14,19]. The lack of ductility was expected, with the microstructure of the consolidated Ti-6Al-4V, Fig 14, containing a large fraction of plate-like alpha phase and only small domains of intergranular beta phase. There is evidence in Fig. 14 that the brittle α-phase laths redefine their shape by brittle fracture of surface protrusions, while the ductile β-phase domains deform plastically to accommodate their neighbouring particles.

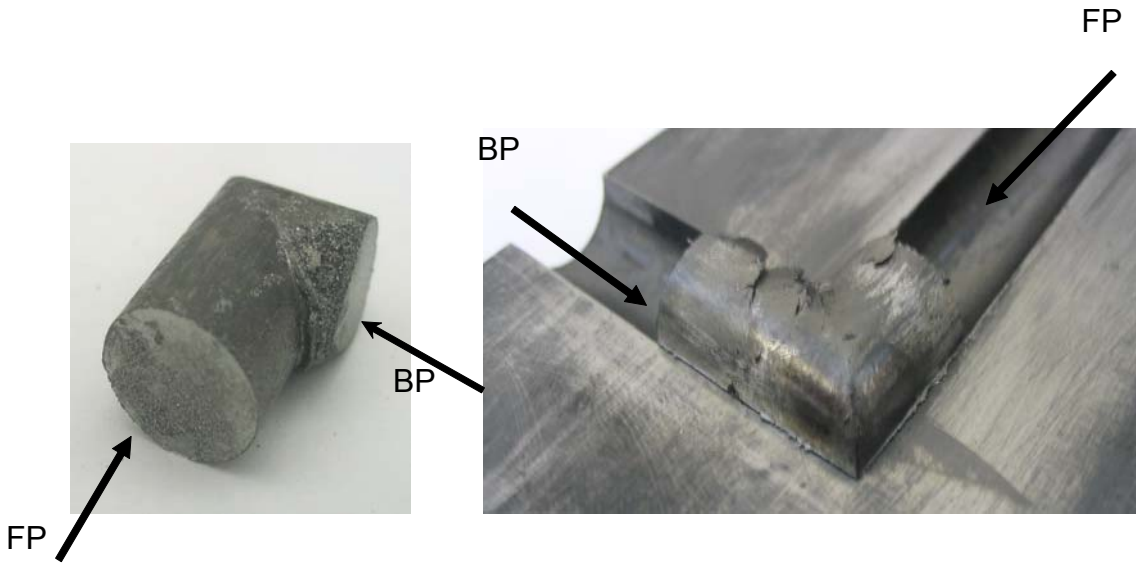

Fig. 13 ECAE with 175 MPa of back-pressure at room temperature
(a) – pre-compaction in the vertical channel; (b) – ECAE processed sample

As shown in [12], relative particle motion contributes significantly to early stage densification or packing. The mechanisms for densification during these early stages include complex interactions as neighbouring particles deform against each other and subsequently increase the interfacial area of contact. The role of ECAE in improving the relative density of the pre-compact is associated with additional fragmentation, mechanical interlocking and realignment of particles, which are all triggered by severe shear deformation. The reduction in the porosity due to shear deformation can be clearly observed qualitatively by optical microscopy, as shown in Fig. 15. Alignment of large particles and fragments of fractured particles filling the spaces between geometric irregularities can be seen from the optical micrograph of the ECAE processed compact processed at 262 MPa of back pressure and shown in Fig. 16

As shown in [12], relative particle motion contributes significantly to early stage densification or packing. The mechanisms for densification during these early stages include complex interactions as neighbouring particles deform against each other and subsequently increase the interfacial area of contact. The role of ECAE in improving the relative density of the pre-compact is associated with additional fragmentation, mechanical interlocking and realignment of particles, which are all triggered by severe shear deformation. The reduction in the porosity due to shear deformation can be clearly observed qualitatively by optical microscopy, as shown in Fig. 15. Alignment of large particles and fragments of fractured particles filling the spaces between geometric irregularities can be seen from the optical micrograph of the ECAE processed compact processed at 262 MPa of back pressure and shown in Fig. 16

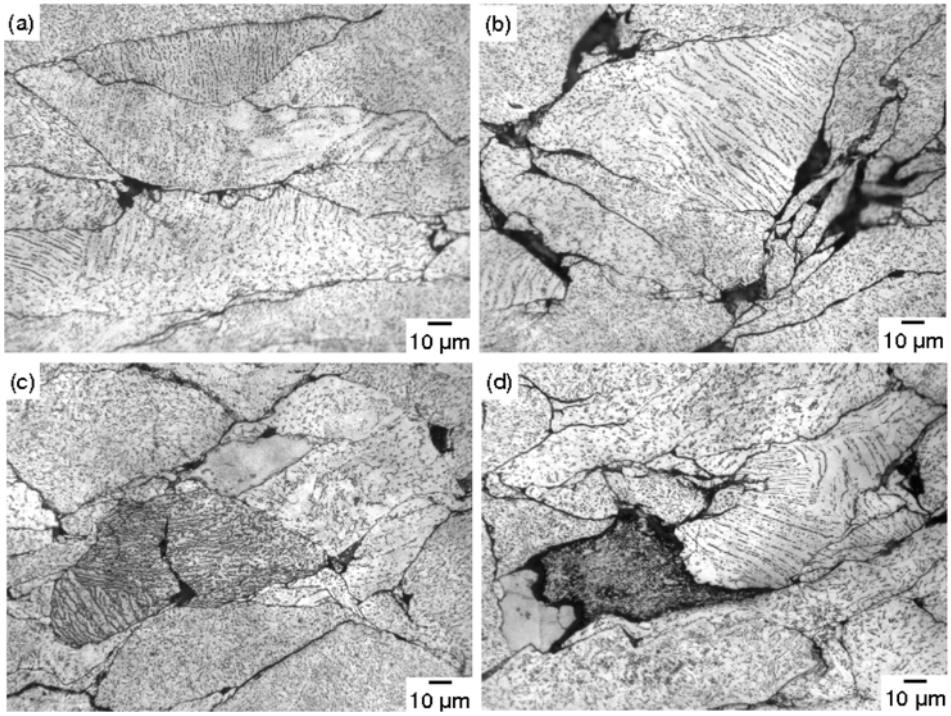

Fig. 14 Optical micrographs of powder processed by ECAE with 175 MPa of back-pressure at room temperature

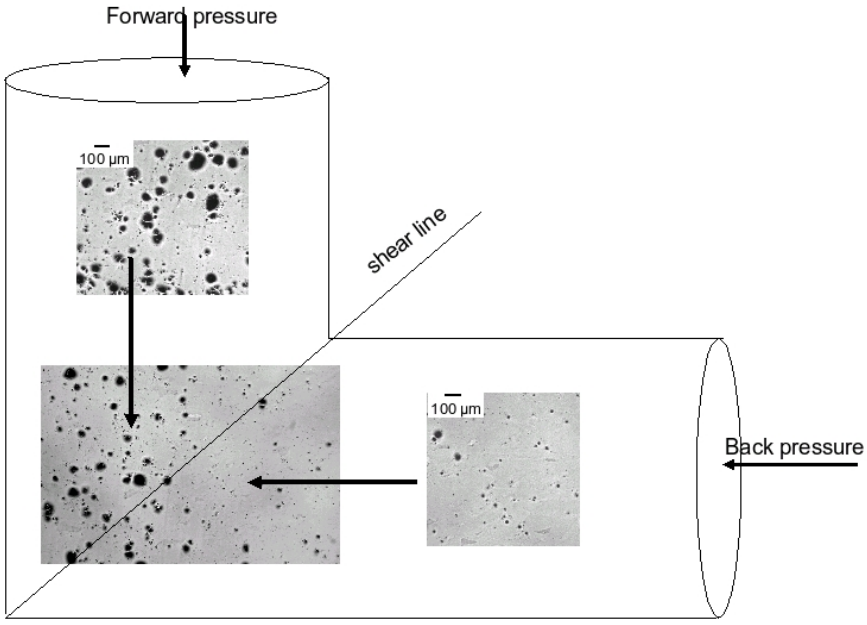

Fig. 15 Influence of shear on pore size and distribution as revealed by optical microscopy.

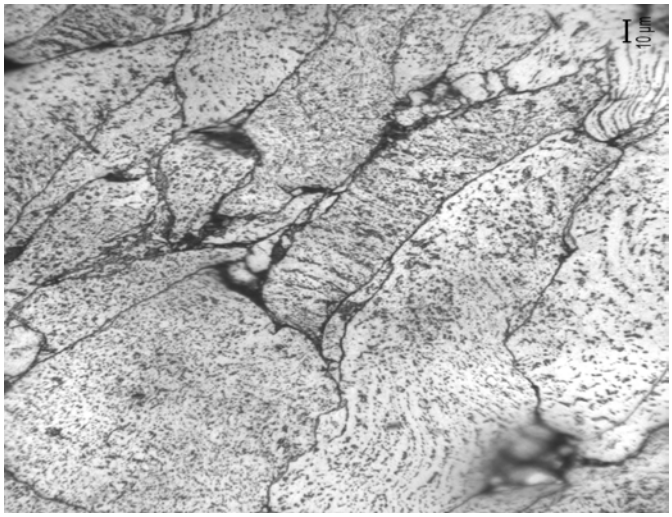

Fig. 16 Realignment of large and fragmented particles after ECAE with 262 MPa of back-pressure at room temperature

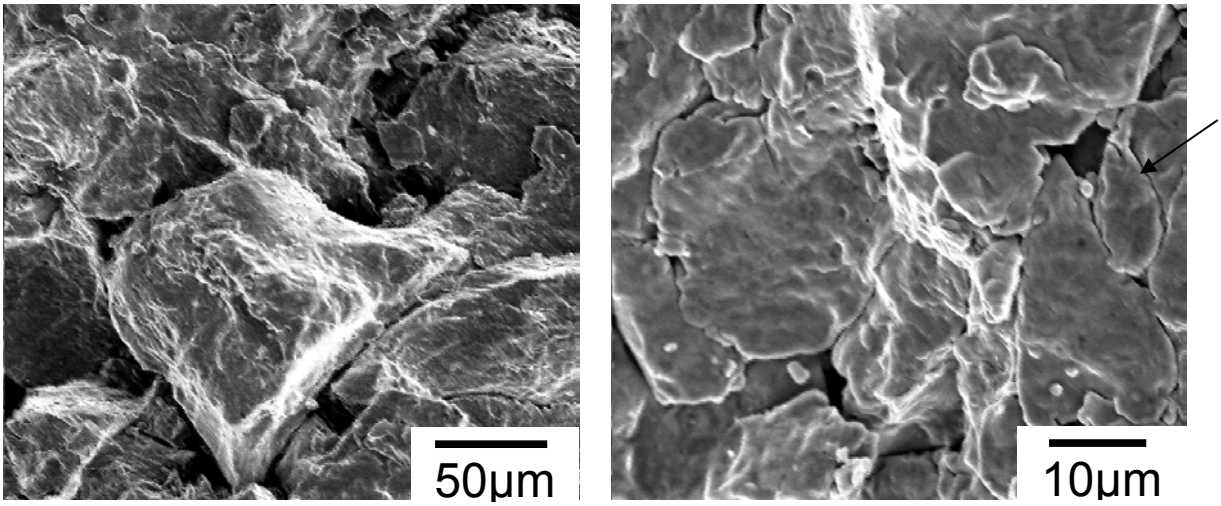

Fig. 17 SEM images of powder processed by ECAE with 175 MPa of back pressure at room temperature

The structure of the billet processed by ECAE with 175 MPa of back pressure at room temperature is shown in the SEM micrographs of Fig. 17. The surfaces have been exposed by fracture of samples from the billett. The consolidated specimen clearly includes particles that were deformed by contact with neighbouring particles and, in interactions between small and large particles, the smaller particles are deformed more severely than the larger particles. In many cases, as illustrated by the small particle arrowed in Fig. 17, the deformation of the smaller particle was apparently more severe than the surrounding larger particles, based on the likely change of shape. The difference in the relative deformation of large and small particles suggests a compaction mechanism involving rigid body motion of large particles or groups of particles, facilitated by preferential deformation of smaller particles, with a net positive influence of pore closure.

Despite the increasing relative density of the compact to a value of 95.6%, the green strength was extremely low (below 100 MPa) as no diffusion bonding had occurred at the particle interfaces.

6.2 Influence of ECAE Temperature on Compaction of Ti-6Al-4V Powder

Improvements in strength and relative density by ECAE can be achieved by promoting self-diffusion at the particle interface through increasing temperature and increasing hydrostatic pressure induced by back pressure. The increase of hydrostatic pressure leads to increasing contact area between the neighbouring particles, thus increasing potential areas for diffusion bonding.

6.2.1 Estimation of self-diffusion at low temperatures

The temperature and hydrostatic pressure dependence of the self-diffusion coefficient, *D*, for Ti in α-Ti may be calculated using an Arrhenius equation of the form:

$$D = D_0 \exp\left(\frac{-Q}{RT}\right) \tag{2}$$

where: D_0 = 6.6 x 10^{-5} cm^2 s^{-1} and *Q* is an activation energy that has components attributable to temperature, Q_T = *169.1 kJ/mol*, and hydrostatic pressure, Q_{HP} [20], where:

$$Q_{HP} = \left(P + \sigma_y / \sqrt{3}\right)\cot\left(\frac{\Phi}{2}\right)\Omega \tag{3}$$

where *P* is the level of applied back pressure during ECAE, σ_y is the tensile yield strength of the Ti-6Al-4V at a given temperature T, Φ is the angle of intersection between the entry and exit channels of the ECAP die, and Ω is the atomic volume = 3.46 x 10^{-29} m^3. The total activation energy Q at a temperature of 400°C and back-pressure of 262 MPa was calculated to be 155.6 KJ/mol. The diffusion coefficient of Ti in α-Ti versus temperature is shown in Fig. 18 for zero and 262 MPa of back-pressure.

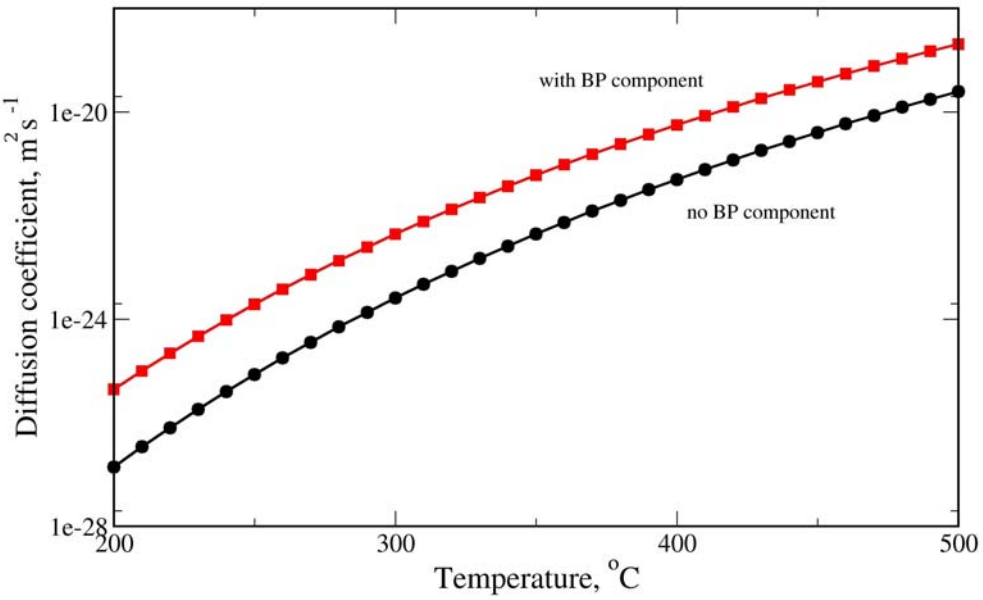

Fig. 18 Self-diffusion coefficient for Ti in α-Ti as a function of temperature at 0 MPa and 262 MPa of back-pressure

Based on an approximate numerical solution to Ficks' second law of diffusion:

$$x^2 / Dt = const \tag{4}$$

where *x* is the distance of mass transport and t is the time of the contact, the distance of mass transport can be estimated. The relationship between squared, normalised diffusion penetration depth and time is plotted in Fig. 19. It can be seen that the mass transport takes longer time in the absence of hydrostatic pressure. Also the increase in temperature from 300ºC to 400ºC significantly decreases the time for mass transport over a given
distance.

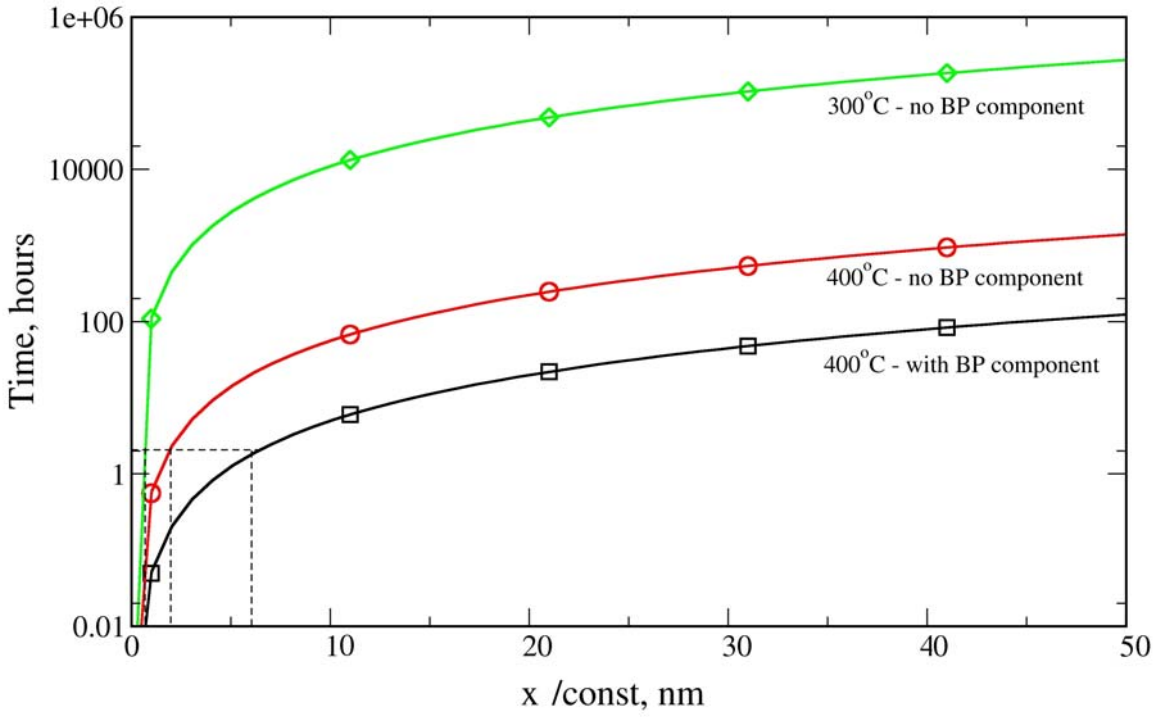

Fig. 19 Time required for penetration by self-diffusion (Ti in α-Ti) plotted as a function of normalised penetration depth, at temperatures of 300°C and 400°C. For the latter temperature, calculations are also included for an example in which a back pressure of 262MPa is applied throughout ECAE.

Taking into account the duration of ECAE processing at 400°C, which is about 2 h including heating and cooling stages, the self-diffusion penetration depth is approximately doubled when a back pressure of 262MPa is applied, compared to that in the absence of back pressure.

6.2.2 Influence of ECAE temperature on cracks in compact

The potential for the ECAE process to produce a compact free of cracking has been studied, while the temperature and back-pressure were increased in steps. At temperatures lower than 400,ºC it was not possible to apply a sufficiently high back pressure to produce a compact without any surface cracks. The influence of the back pressure on the suppression of cracking during ECAE at 400ºC can be seen in Fig. 20.

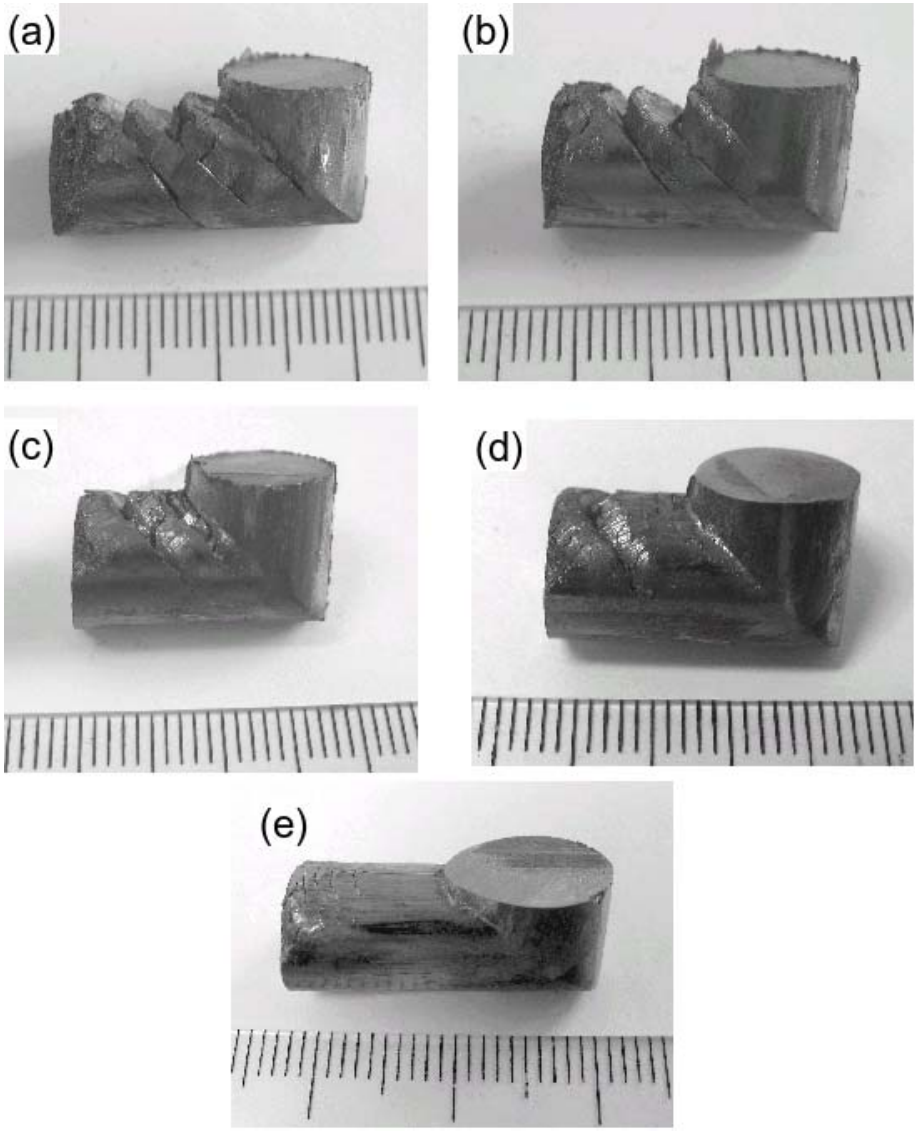

Fig. 20 The appearance of cracking in compacts produced by ECAE at 400ºC with different levels of back-pressure
(a) 21 MPa; (b) 43 MPa; (c) 175 MPa; (d) 262 MPa; (e) 350MPa.

To reduce the tendency for cracking in the consolidated billet, the back pressure was increased systematically from 21 to 350 MPa. As can be seen in Fig. 20, an increase in back pressure progressively reduces the number cracks in the given length of extruded product and also reduces the extent of the intrusion of the cracks across the billet section. A relative crack length was determined and the influence of back pressure on this relative crack length is shown in Fig. 21. An increase of back pressure to 350 MPa at the temperature of 400ºC was seen to fully eliminate macroscopic cracks in the compact, but there was still some evidence of surface cracking particularly at the leading end of the billet.

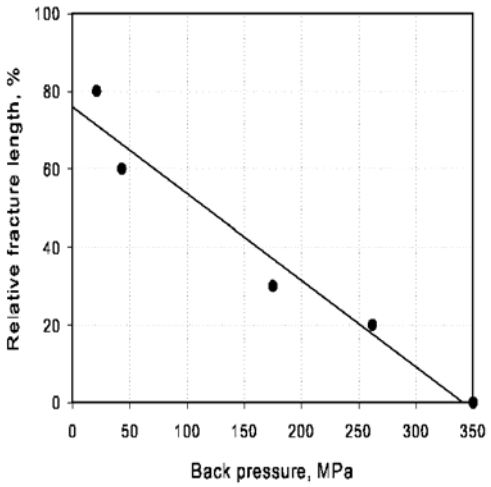

Fig. 21 Relative crack length as a function of back-pressure for compacts produced by ECAE at 400ºC

6.2.3 Influence of ECAE temperature on relative density of compact

The increases in relative density observed with increasing temperature and back-pressure are shown in Fig. 22.

For values of back pressure of 175MP. and above, the compact density obtained at room temperature (RT) of ~95.3% was observed to increase to ~98.3% with an increasing in temperature to 400ºC. Low values of back pressure were seen to have a large impact on densification, whereas at larger values of back pressure the density achievable saturates. For a given temperature, the density increases from ~95% to in excess of 98% for levels of back pressure in the range of 0-175 MPa, while for back pressures in the range of 175-350MPa the relative densities achieved remain almost constant. This conclusion will be later checked for higher values of back pressure, which become possible when friction between the charge and the die channel wall is reduced by compaction of the charge in a tube skin.

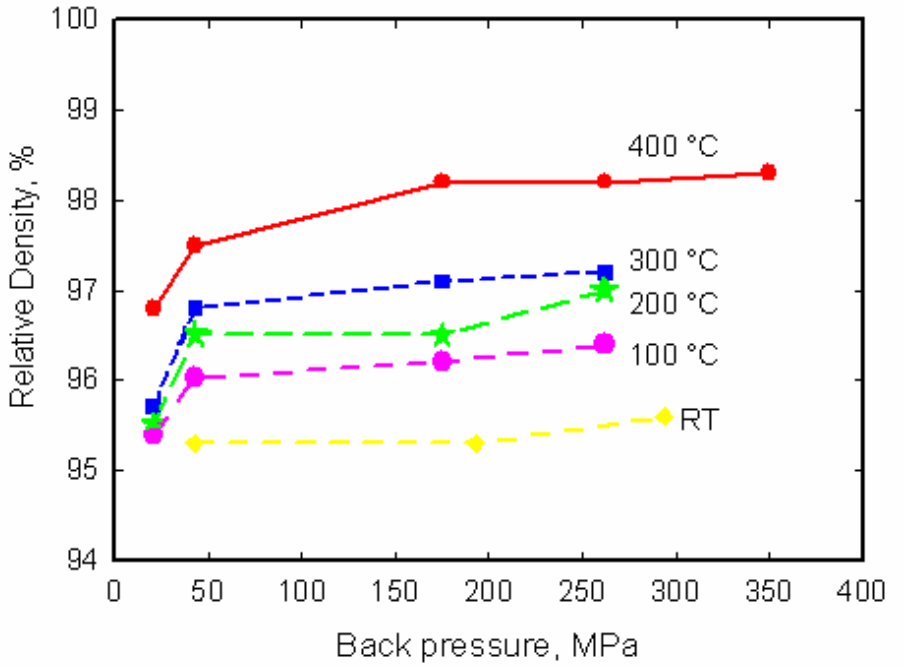

Fig. 22. Relative densities of the compacts produced by ECAE as a function of back pressure for various processing temperatures.

Comparison of the microstructures of billets produced at different temperatures, but with a similar level of back pressure of 175 MPa is shown in Fig. 23. The images show that an increase in the temperature of ECAE processing above the room temperature reduces significantly the scale of the remaining pores to below a few microns.

It appears that the densification efficiency primarily depends on the balance of forward and back pressures and temperature. However, there are several other factors that may have an effect including inhomogeneity in the internal friction between particles, the frictional stress between the extruded segment and the exit channel, and the frictional stresses between the particles and the entry channel. To further increase the relative density would require a further increase in the value of back pressure. However, at this level of back-pressure (using dry lubrication) and the current equipment design, the forward pressure reaches the limit, which the punch and the ECAE die can withstand without fracture. The high forward pressure requirement is in part due to the increasing friction, which increases in proportion to the level of back pressure. Therefore, to significantly increase the back pressure, without increasing in a forward pressure, friction must be reduced, and these efforts will be described in further paragraphs.

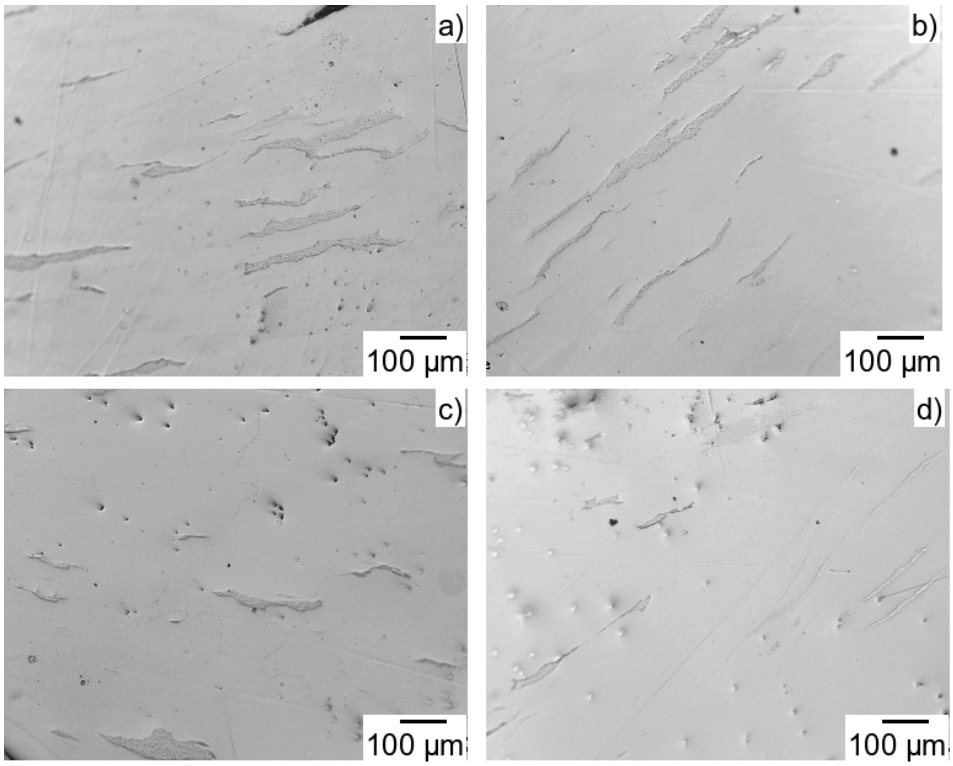

Fig. 23 Optical micrographs of compacts processed by ECAE with 175 MPa of back pressure at temperatures of:
(a) 100 ºC; (b) 200 ºC; (c) 300 ºC; (d) 400 ºC

Comparison of optical micrographs of billets produced at room temperature and 400ºC is shown in Fig. 24. A decrease of exposed pore area, from 8.5% for billets processed at RT to 0.5% for those processed at 400ºC, was observed. This trend is also consistent with density measurements obtained by Archimedes' method, Fig. 22. The increase in particle ductility anticipated at 400ºC results in a more elongated shape for the particles parallel to the shearing direction, as shown in Fig. 24(c,d). The most geometrically difficult pores to close are those formed at triple junctions between the particles. A critical level of ductility is required to close these pores and this was obtained at temperatures above 300 ºC, as is illustrated in Fig. 25.

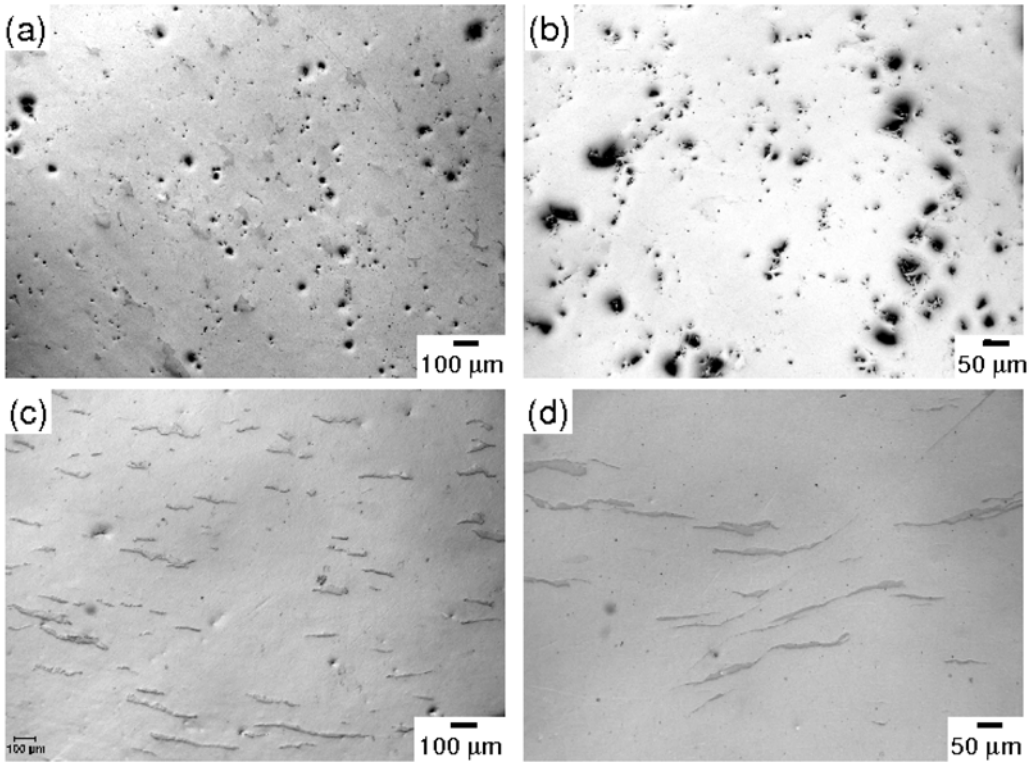

Fig. 24 Optical micrographs of billets processed at different conditions.
(a) (b) at RT with BP = 87MPa (two different magnifications);
(c) (d) at 400°C with BP =175 MPa (two different magnifications)

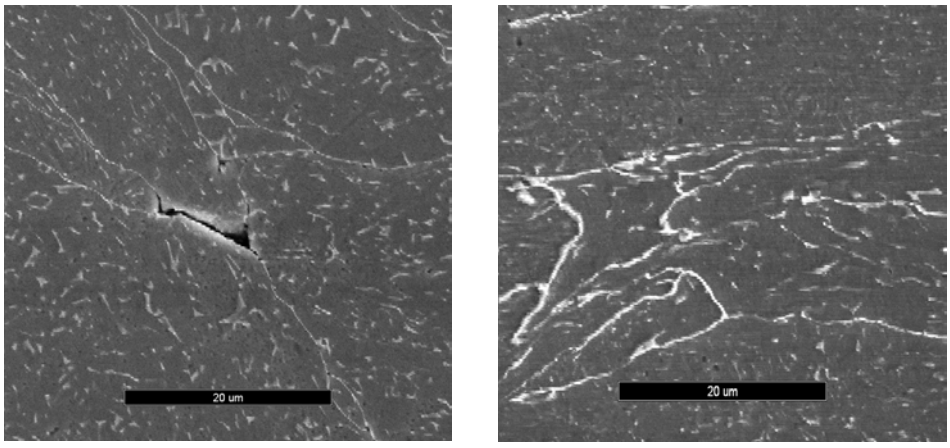

Fig. 25. SEM images of compacts produced at room temperature and 400ºC showing particle triple junctions.

6.2.4 Influence of ECAE temperature on Vickers hardness of compact

Fig. 26 shows the Vickers hardness as a function of back pressure and temperature. A slightly increase of HV was observed with back pressure for each temperature of ECAE processing. Hardness increased also with processing temperature, rising from room temperature to 300 ºC. However, the hardness of compacts produced by ECAE at 400ºC, was lower than the hardness of those produced at 300 ºC for all levels of back pressure. This can be explained by micro-strain relaxation due to twin activity at elevated temperature. Evidence in support of this explanation was observed by TEM and this will be discussed in Section 6.8.

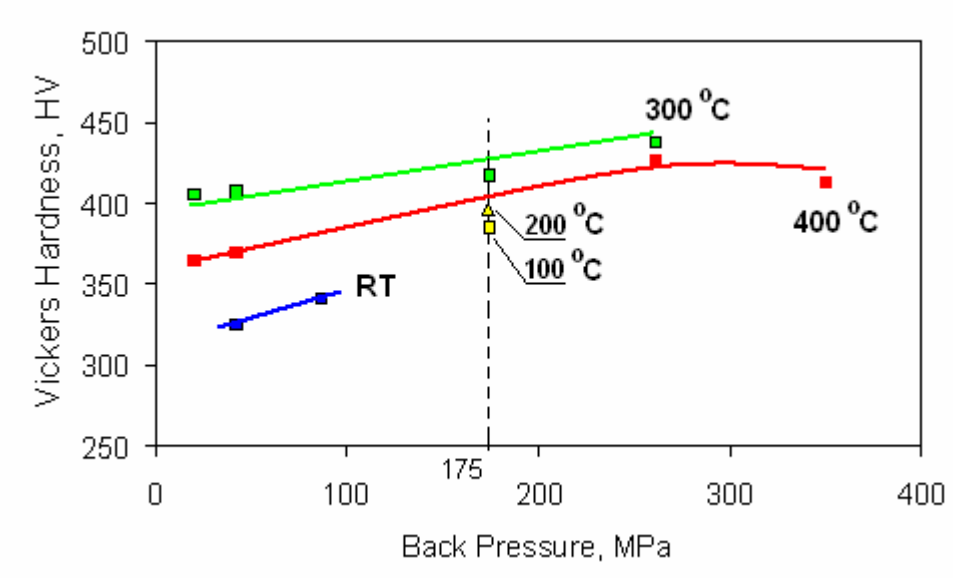

Fig. 26 Vickers hardness as a function of back pressure and temperature

Shear deformation plays an important role in hardness development. Hardness measurements recorded from a sample produced by ECAE at 300ºC, before and after the shear plane, revealed an approximate doubling of hardness from 152 and 226HV to 319 and 429HV respectively, for back pressures of 200 and 300MPa respectively. This can be explained by the significant number density of non-closed pores present in the sample before the shear line. The role of shear strain in densification will be discussed in Section 6.4.

6.2.5 Influence of ECAE temperature on green strength of compact

The green strength of the compacts produced at room temperature was extremely lowl. A relatively high density of ~95% was obtained by better pre-packing before the shear line under high hydrostatic pressure followed by shear deformation leading to apparently brittle fracture of surface protrusions, changes of shape and realignment of

particles with improved mechanical interlocking. As the temperature of ECAE processing wasincreased, the green strength of the compacts increased, Fig. 27

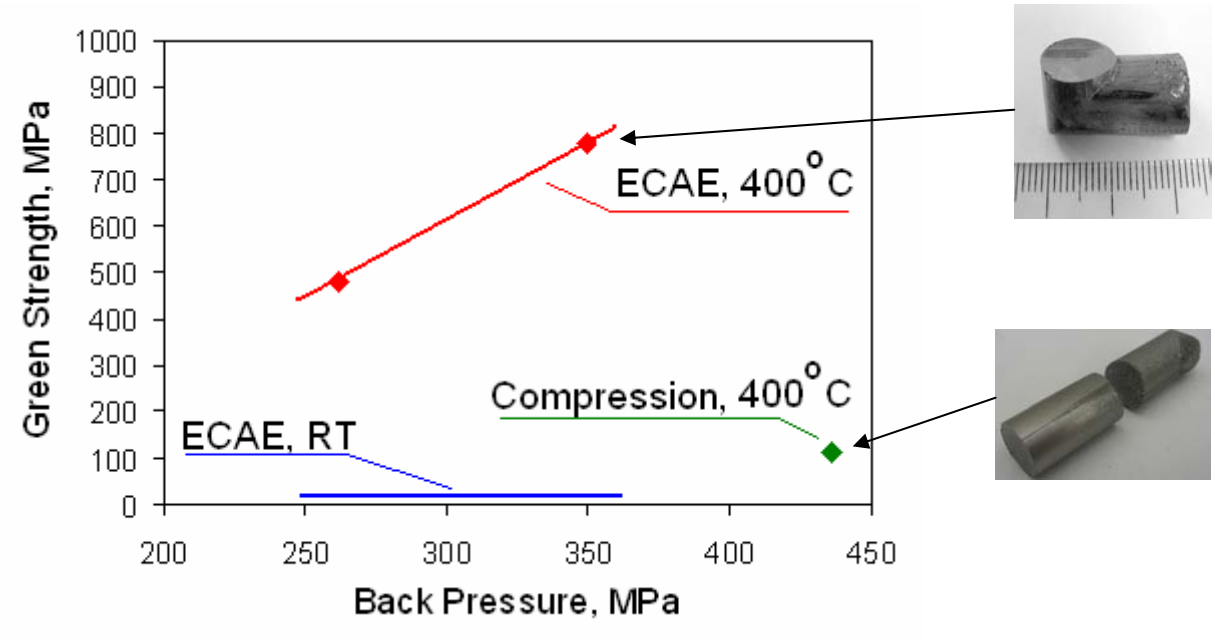

Fig. 27 Green strength versus back pressure for compacts produced by ECAE at RT and 400ºC, and for a sample produced by direct compaction.

6.3 Influence of Encapsulation on Relative Density and Hardness of Compact

To investigate the relative density and hardness of compacts at higher levels of back-pressure, the friction was eliminated by encapsulating the powder in aluminium tubes (9mm inner diameter, 10 mm outer diameter) and using a wet lubricant (graphite based grease). The results on density and Vickers Hardness are summarized in Table 3. It seems that introduction of encapsulation of the powder in soft-metal tubes does not improve the relative density of compacts.

There are two reasons for this:

1. The packing density of the powder in the aluminium tube or when using wet lubricant is not as high as that obtained in the entry channel of ECAE die, and therefore, buckling of the thin aluminium tube begins immediately as the forward pressure is applied. This buckling creates the stress concentrators at the surface where compacts crack and relative density is, therefore, low.

2. The high friction levels, when tubes and wet lubricant are not used, create an additional (non-accountable) component in hydrostatic pressure which results in better relative density. Interestingly that sample number 8 which was pre-compacted by better technique have shown improvement in relative density. However, such pre-compaction is time consuming and can not be considered as valuable industrial option.

Table 3 Relative density and Vickers hardness of billets processed by ECAP at 400ºC.

No	BP, MPa	Relative Density, %	HV
ECAE compaction without Al tubes			
1	43	97.4	369
2	175	98.1	371
3	262	98.2	426
4	350	98.3	412
ECAE compaction with Al tubes			
5	350	97.4	415
6	393	97.8	419
7	436	97.6	438
8*	480	98.6	431
ECAE compaction with wet lubricant			
9	350	97.3	421
10	436	97.4	426
11	524	97.8	428

The relative density and Vickers Hardness of compacts produced by ECAE at 400ºC using aluminium tubes as functions of back pressure is shown in Fig. 28. Comparison of relative density for compact produced with wet lubricant, with and without Al tubes is shown in Fig, 29.

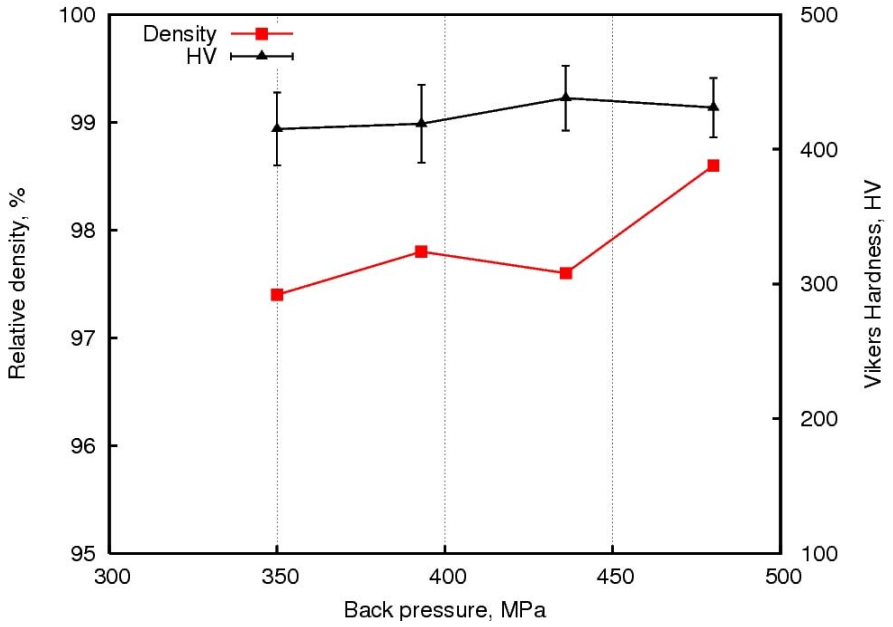

Fig. 28 Relative density and Vickers Hardness vs. back pressure (compacts produced using powder encapsulation in aluminium tubes)

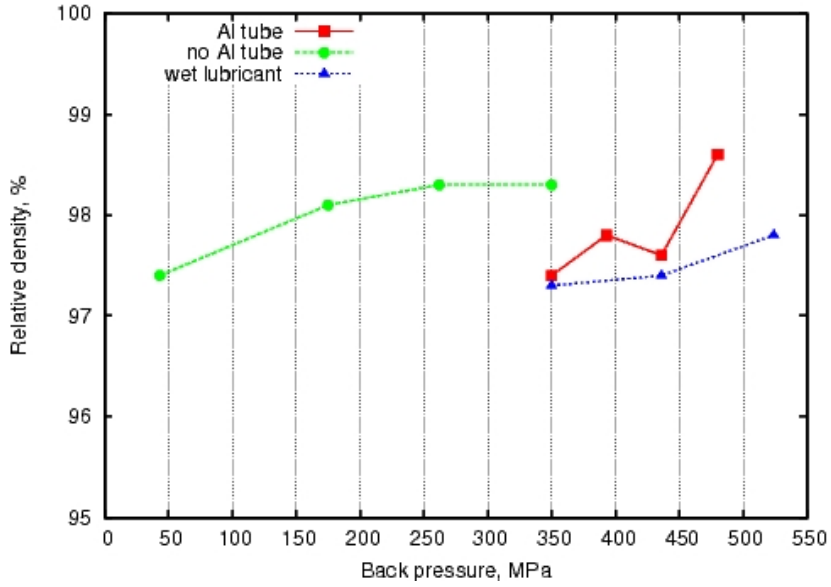

Fig. 29 Relative density vs. back pressure of compacts produced by ECAP with and without aluminium tubes.

Experiments with aluminium tubes show that possible increase in back-pressure above 350-400 MPa is expected to lead to another gain in relative density. However, that will require a redesign of the ECAE die to allow higher loadings on the forward punch. For current die design it was not possible to increase further the hydrostatic component without eliminating friction by use of the aluminium tubes or wet lubricants.

6.4 Influence of Shear Strain on Densification

Pore closure and a change of pore shape under shear deformation and hydrostatic pressure experienced in ECAE was studied in our previous work [21] for a range of initial pore sizes and orientations. The deformation of a single pore, Fig. 30, can be presented as a change in the shape and a change in the volume. If the level of hydrostatic pressure is sufficiently high the walls of the pore could be welded after closure. Simple shear deformation helps to change the geometry of the pore to one favorable for closure under hydrostatic pressure, Fig. 30.

A comparison study of conventional compaction and ECAE compaction was carried out at the temperature of 400ºC. Conventional compaction (shown in Fig. 27) has been performed in a closed die. The parameters of compaction and the results on the relative density, Vickers Hardness and Green strength are listed in Table 4. It can be noticed that shear deformation improves the relative density by about 2-2.4%, hardness by 40-75 HV, and green strength 4-7 times. The role of hydrostatic pressure at the temperature of 400ºC is very significant in enhancing diffusivity as discussed in Section 6.2.1, which subsequently results in significant increase in green strength of the compact to the level beyond 700 MPa.

Table 4. Characteristics of compacts produced at 400 ºC by direct compression in closed die and by ECAE

Properties	Conventional Compaction		ECAP Compaction	
Designation of compact	B1	B2	B3	B4
Hydrostatic Pressure, MPa	2500	3100	2500	3100
Relative Density, %	95.8	96.4	98.2	98.3
HV	351	373	426	412
Green Strength, MPa	110	102	480	747

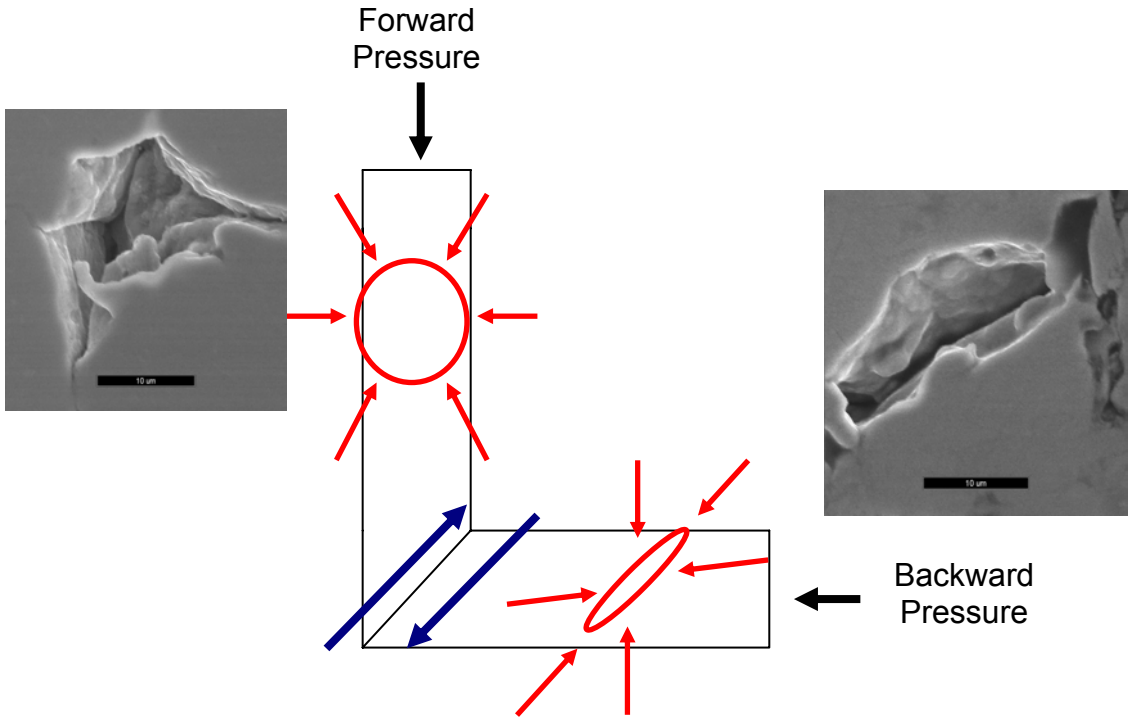

Fig. 30 The schematic of pores closure and SEM images of powder compact exemplifying pore shape change.

Optical microscopy of conventionally compacted billets Fig. 31a, b revealed a certain amount of voids compare to compacts produced by ECAE Fig. 31c, d, which is consistent with the relative density measurements. The elimination of pores by ECAE especially at triple junctions of the particles, and the change of their geometry to one more favourable for closure elliptical shape is clearly illustrated in these micrographs. There is no such effect by using conventional direct compaction in a closed die.

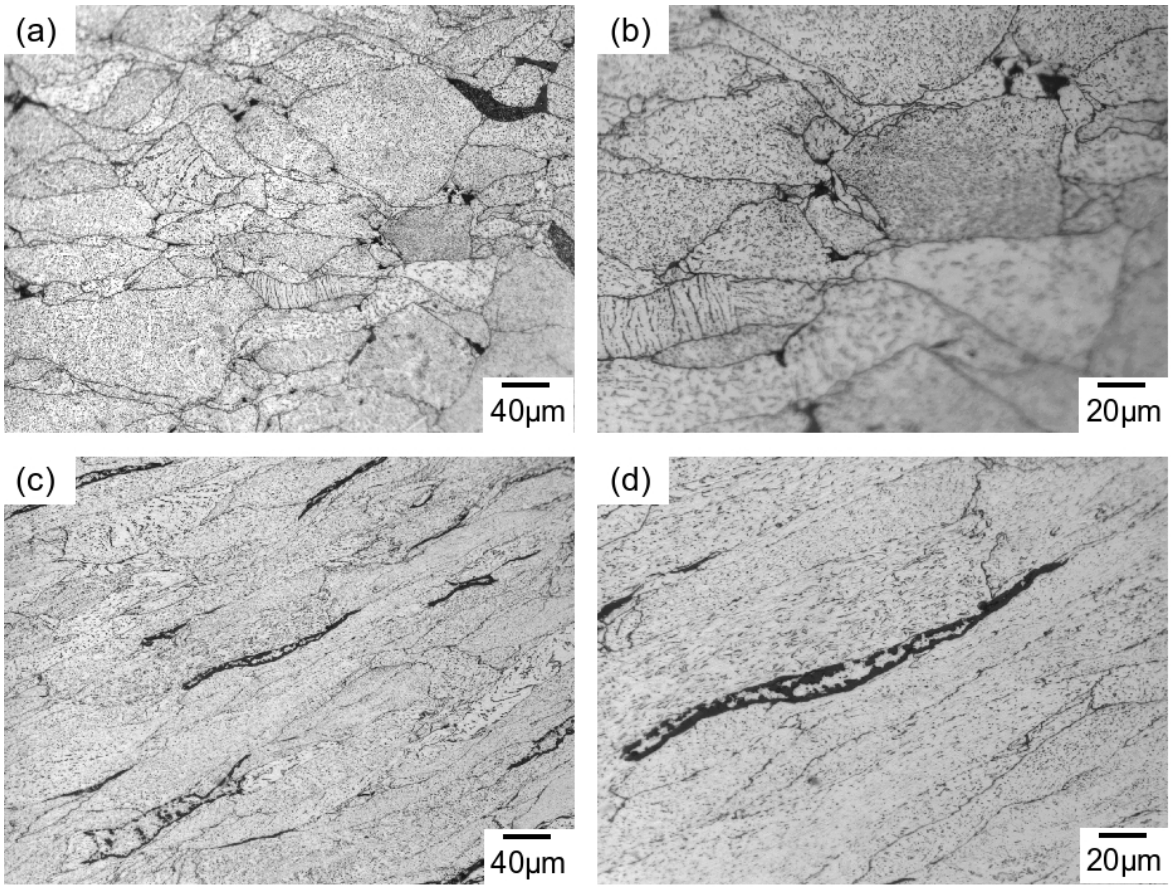

Fig. 31 OM micrographs of billet compressed at 400 °C (a), (b) by direct compaction and (c), (d) by ECAE (two different magnifications).

6.5 Role of the Second ECAE Pass

The necessity of a second pass of ECAE and its possible influence on relative density has been studied. Two passes of ECAE with 262 MPa of back-pressure and at the temperature of 400 ºC were performed using route C (flipping sample 180º between passes). As can be seen from the Table 1 (samples 37-39) the relative density was slightly higher after second pass by about 0.5%, and the OM micrographs show no porosity, Fig. 32 a, b. However the ductility of the compact produced in the first pass was not high enough to withstand 115% of deformation in the second pass. Additional micro-cracks were forming on the surface during the second pass as can be seen in the SEM micrographs o their under-surface layer, Fig. 33a,b. Considering also the economic disadvantage of a second pass, it was concluded that one pass of ECAE with a high level of back-pressure is the optimal condition for obtaining high density compacts.

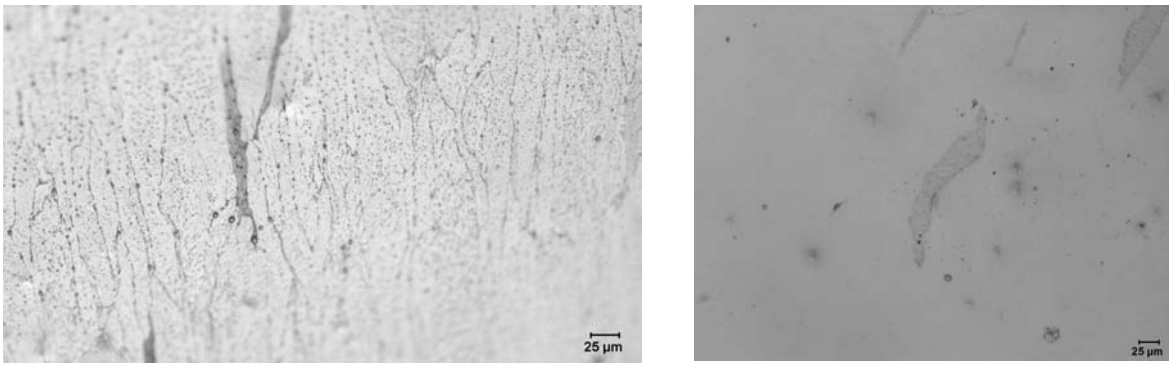

a b

Fig. 32 OM images of the compact after two passes of ECAE at 400 ºC with 262 MPa of back-pressure
(a) – etched structure; (b) – un-etched structure

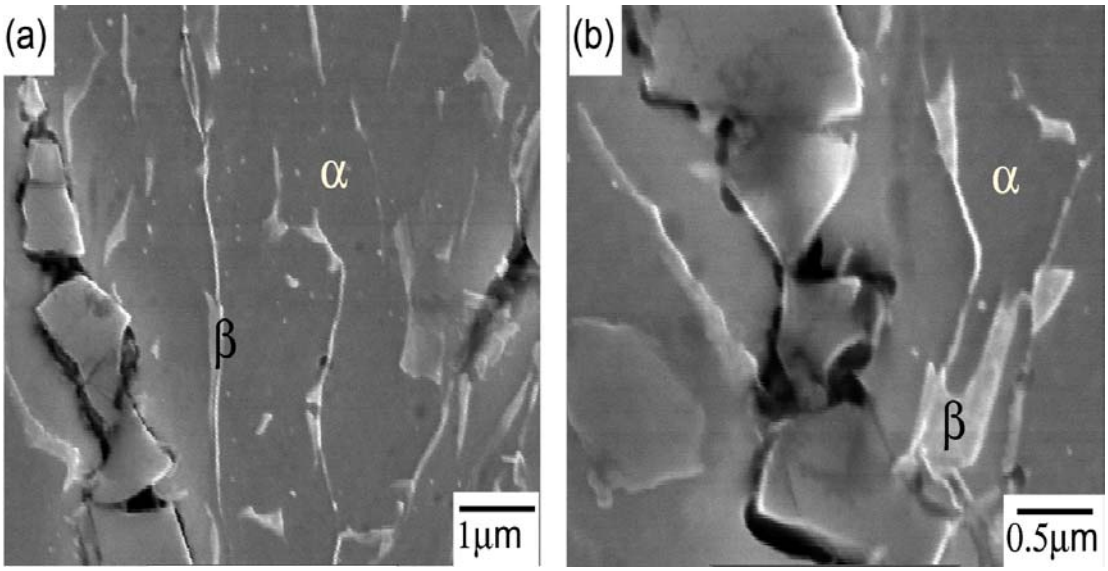

Fig. 33 SEM micrographs of micro-cracks in compacts produced by two ECAE passes at 400ºC and 262 MPa of back-pressure.

6.6 Role of the Holding Time after ECAE Compaction

The influence of a holding time, at preset temperature and pressure, after the ECAE pass, on the relative density has been investigated. Samples processed by ECAE at 400ºC and back-pressure of 262 MPa were held in the exit channel under these pressure and temperature conditions for 1 hour. The relative density did not

substantially improve, as the holding time was not long enough to enhance significantly the mass transport distance (see Section 6.2.1). The holding times and temperatures required to recover the remaining porosity by surface diffusion are out of the scope of the project. Furthermore, the TEM observation of the microstructure after holding the billet for 1 hour at 400°C reveals a decrease in the density of deformation twins and. dislocations inside the grains, which will be shown in Section 6.8 to play an important role in densification.

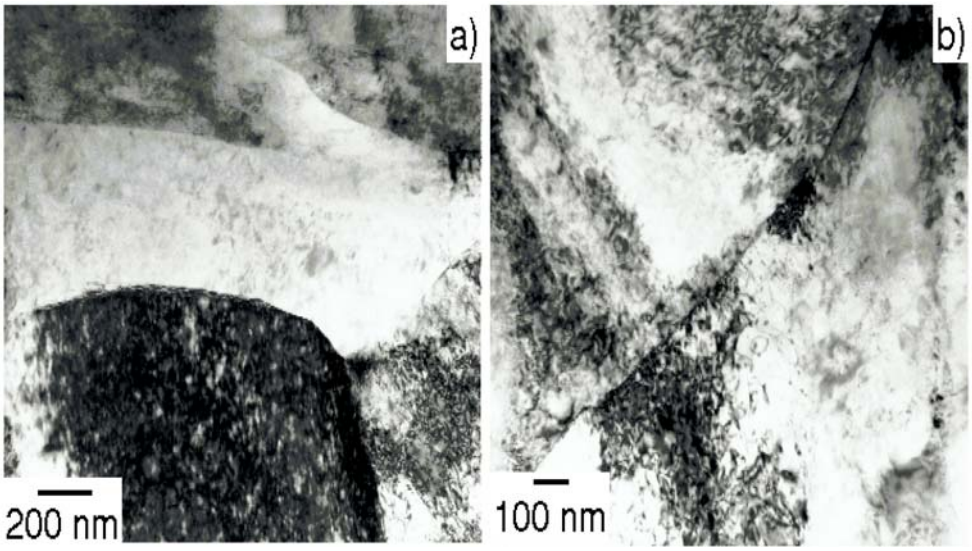

Fig. 34 TEM micrographs of compact produced at 400ºC by ECAE with 262 MPa of back-pressure and held for 1 hour under pressure and temperature.

6.7 Sintering after ECAE Compaction

The influence of post ECAE sintering has been investigated by heat treating, at 1100° C for 4 hrs, the billet processed by ECAE with a back-pressure of 262 MPa at the temperature of 400ºC. The TEM micrographs are shown in Fig. 35. A fully recrystallized structure can be observed. In Fig 35a, α – phase and ß – phase are shown, and in Fig. 35b only α – phase can be seen. The dark curves in Fig.35b correspond to the Bragg reflection which occurs due to the local shape of the foil.

The relative density of the billet has been increased by 0.4-0.8% due to sintering and the relative density of 98.7% has been reached. Correspondingly, Vickers Hardness after sintering decreased from 420 to 340 HV due to annihilation of the dislocations and subsequent decrease of dislocation density, Fig. 36.

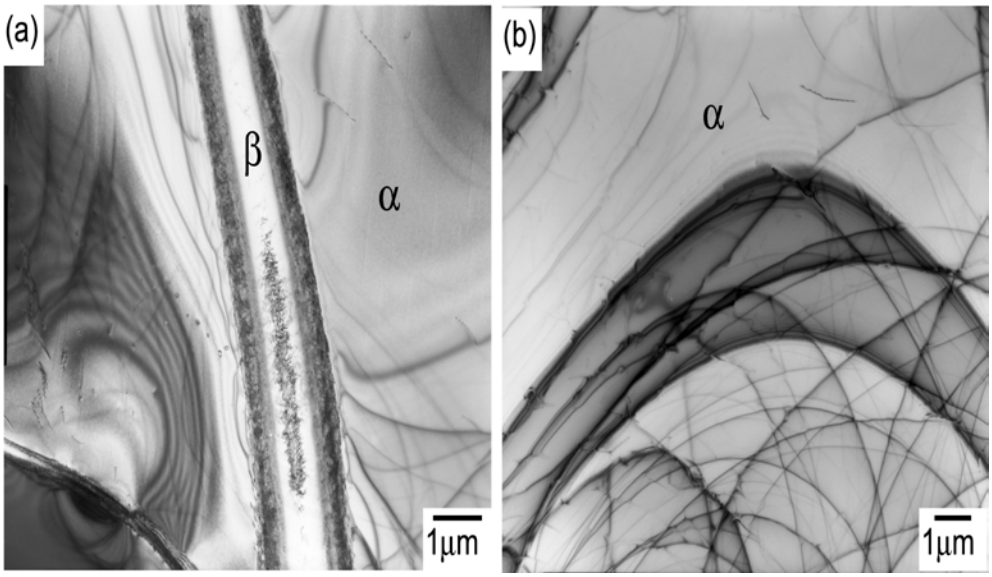

Fig. 35 TEM micrographs of billet processed by ECAE with 262 MPa at 400ºC and sintered at 1100ºC for 4 hrs (α- and ß-phases) .

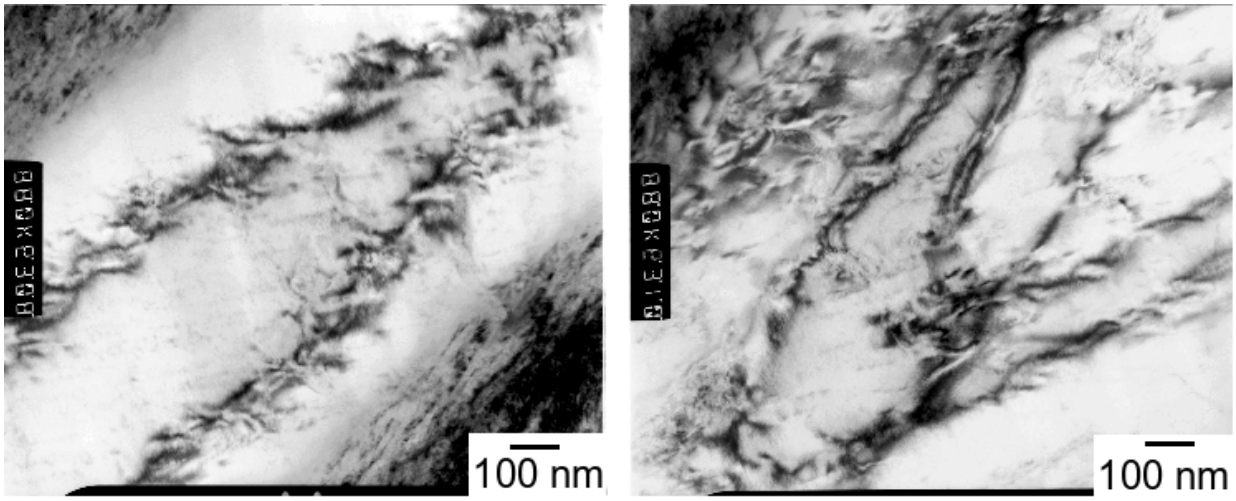

Fig. 36 TEM micrographs of billet processed by ECAE with 262 MPa at 400ºC and sintered at 1100ºC for 4 hrs (microstructure relaxation).

6.8 Improvement of Compaction due to Change in the Deformation Mode

It is expected that the improvement of compaction by ECAE is due to change of the deformation mode, which triggers different physical mechanisms in material.

6.8.1 Crystallite size and microstrain measured by XRD analysis

The crystallite size and lattice microstrain within billets produced by ECAE with

various back pressure at 400°C were determined by measuring the deviation of XRD line profile of as-received powder using the Scherrer and Williamson-Hall equations. The XRD measurements of Ti64 powder in as-received condition and after ECAE are shown in Fig. 37. The peaks broaden as the back pressure increases from 21 MPa to 350 MPa.

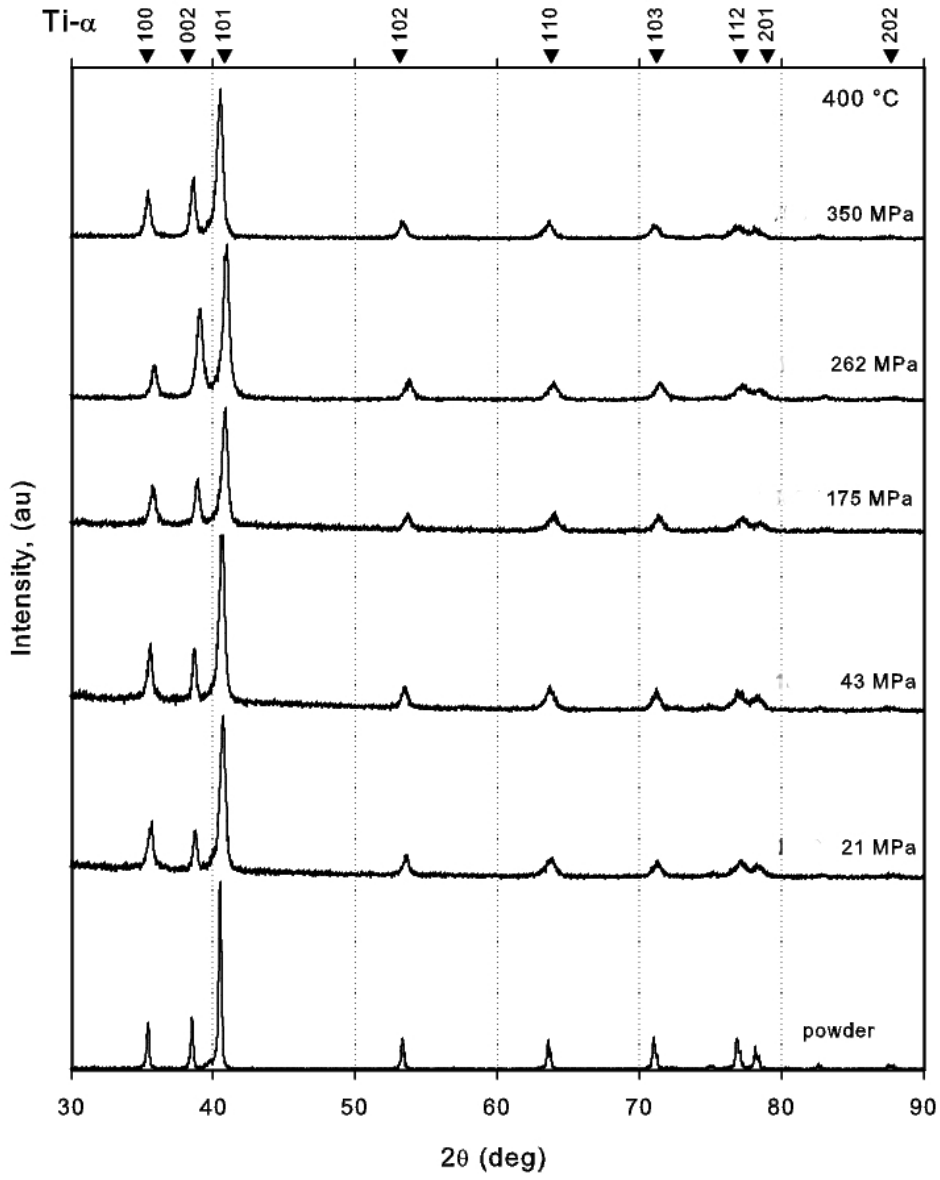

Fig. 37 XRD measurements of Ti64 powder and billets processed by ECAP at 400ºC.

.

Both equations were employed as the Scherrer equation underestimates the grain size as a result of neglecting the micro-strain components. The first four peaks (100), (002), (101) and (102) were used to determine the grain size and micro-strain.

The crystallite dimension, ***t***, averaged over volume according to Scherrer equation is:

$$t = \frac{K \cdot \lambda}{B \cdot cos\theta} \tag{4}$$

and according to Williamson-Hall equation::

$$\frac{B \cdot cos\theta}{\lambda} = \frac{K \cdot \lambda}{t} + 2 \cdot \frac{\Delta d}{d} \cdot \frac{sin\theta}{\lambda} \tag{5}$$

where K =0.9, λ is Cu wave length and B is Full-Width Half-Maximum (FWHM).

The crystallite size as a function of back-pressure applied is plotted in Fig. 38. As can be seen, there is a tendency for underestimation for the crystallite size by about 10-15 nm as a results of neglecting the micro-strain component in the Scherrer equation. The Scherrer equation plot indicates the tendency of grain refinement with increasing the back pressure while the Williamson-Hall plot indicates that the average crystallite size of 25 nm was not significantly influenced by back pressure.

Contrary, the relative lattice distortion, Fig. 39, increases from 0.02 to 0.12 % with back-pressure. XRD measurements showed evidence of significant plastic deformation and increased dislocation density, leading to enhanced mass transport consistent with the observed reduction in the size and density of pores. Thus, plastic deformation is expected to induce pores closure.

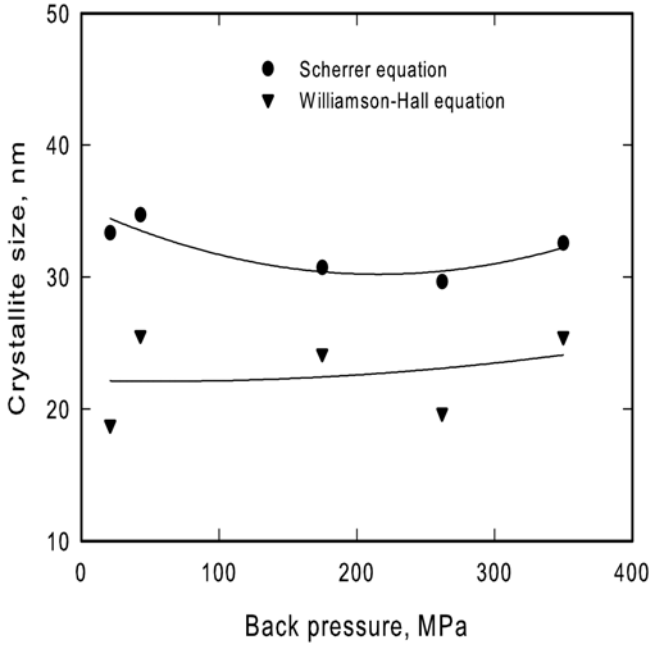

Fig. 38 Crystallite size measured using Scherrer and Williamson-Hall equations.

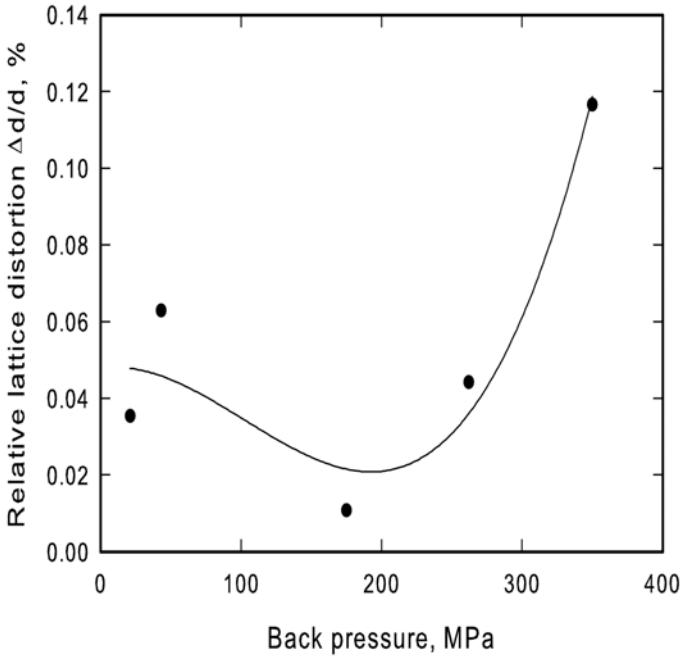

Fig. 39 Micro-strain calculated based on XRD measurements using Williamson-Hall equation.

In addition, the increase in diffusion at 400°C is expected to enhance mass transport to the surface of the pore. The surface energy sustained by the pore is directly proportional to the applied stress and pore radius, and inversely proportional to Young's modulus and surface tension. With increasing stress, the surface tension decreases and the pore cannot sustain local equilibrium, resulting in pore collapse and volume reduction. The combined effect of increased plastic deformation with enhanced diffusion results in significant improvement in the relative density up to 98.3%, a value impossible to achieve before sintering by means of any other mechanical proces

6.8.2 Microstructure evolution by TEM observations

It is well known that due to its limited number of slip systems, plastic deformation of hcp titanium is usually accommodated by a combination of deformation twinning and dislocation slip. At temperatures of 400°C and above, $\{10\bar{1}1\}$ twinning is accompanied by ***a+c*** dislocation slip. Normally deformation twins were not observed in Ti-6Al-4V unless high strain rates were used [22]. However the TEM observation carried out on compacts produced by ECAE at 400ºC revealed multiple twin nucleation and growth.

The present ECAE process was conducted at an extrusion rate of 8 mm/sec corresponding to an approximate strain rate of 1.13 s^{-1}. This value of strain rate is not

conventionally large enough to initiate deformation twins. However, the intensive twinning activity was observed accompanied by dislocation slip mechanism, Fig. 39. The diffraction pattern has been indexed as α -Ti.

The twin bands of different size were observed within this micrograph (double arrow, Fig. 39a) oriented along $(10\bar{1}0)$ plane. They were supposed to be induced by twinning deformation mechanism. Second type of twins, Fig 40b, such as thin lamellar twins induced by slip deformation mechanism were also detected.

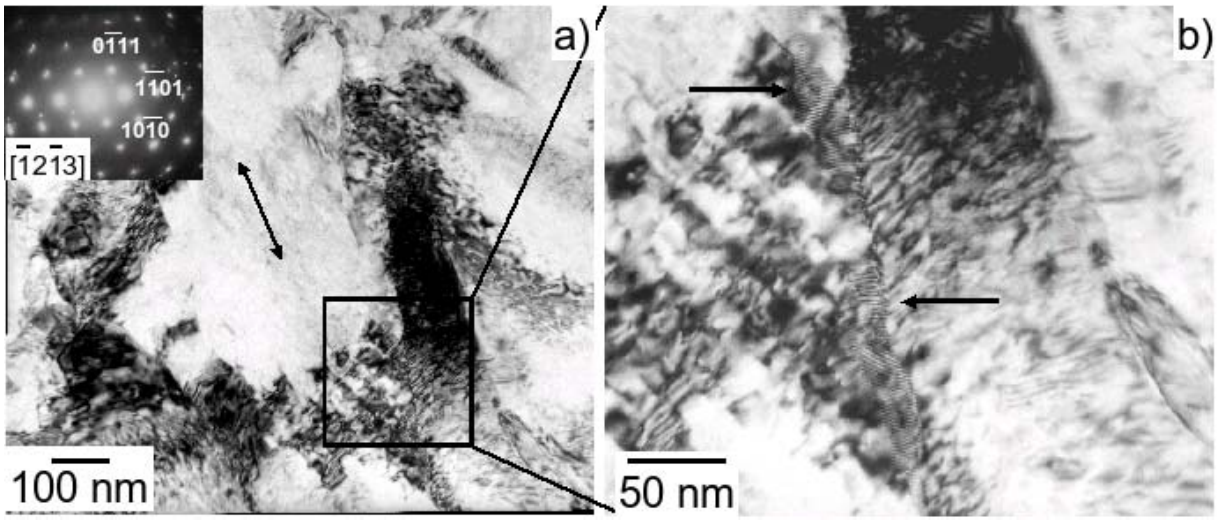

a b

Fig. 40 TEM micrographs of compact produced by ECAE with 262 MPa of back-pressure at 400ºC ((b) is enlargement of squared area in (a) with arrows show twins; double arrow in (a) shows twin bands)

Fig. 41 shows the bright-field TEM image and electron diffraction pattern of billet processed by ECAE with a back pressure of 262 MPa at 400°C. It can be seen, Fig. 39, that due to plastic deformation the shear bands about 20-50 nm wide form within the grains. The network of low angle sub-boundary walls slanting to the shear bands shape the crystallites of 25 nm as defined by XRD measurements. The microstructure is composed of elongated bands of contrast while the diffraction pattern reveals diffuse spots, which suggest that the bands may constitute low angle sub-boundaries. Indexing the selected area, electron diffraction pattern revealed a zone axis of $\left[0\bar{1}11\right]$ α-Ti. Consistent with the XRD analysis, electron microscopy revealed evidence of local lattice distortion and increased dislocation activity, consistent with the mass transport mechanism necessary to encourage pore shrinkage and closure.

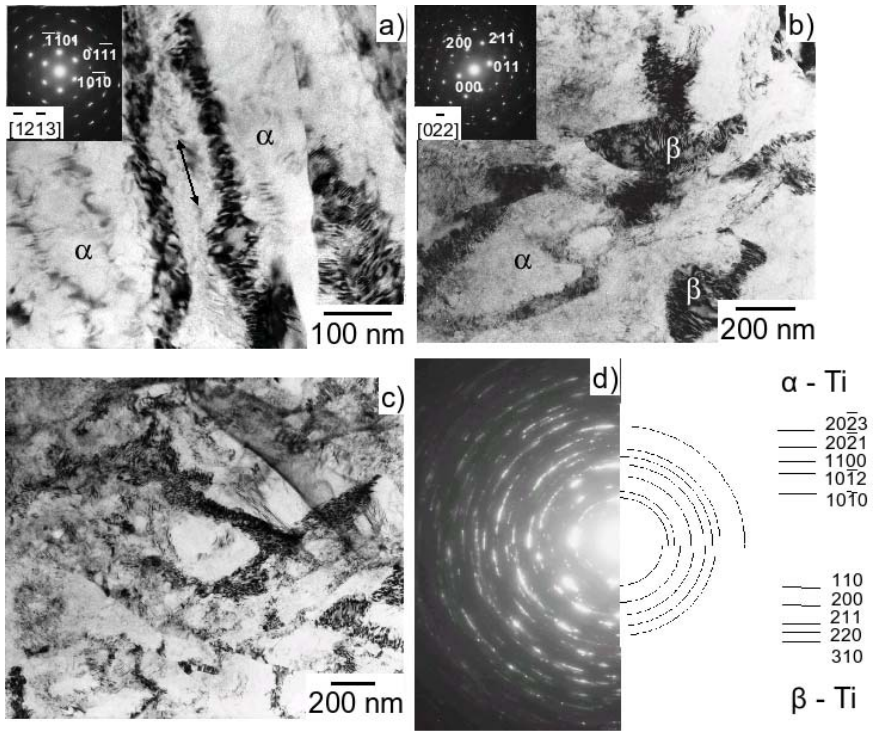

Fig. 41 TEM micrographs of compact produced by ECAE with 262 MPa of back-pressure at 400ºC

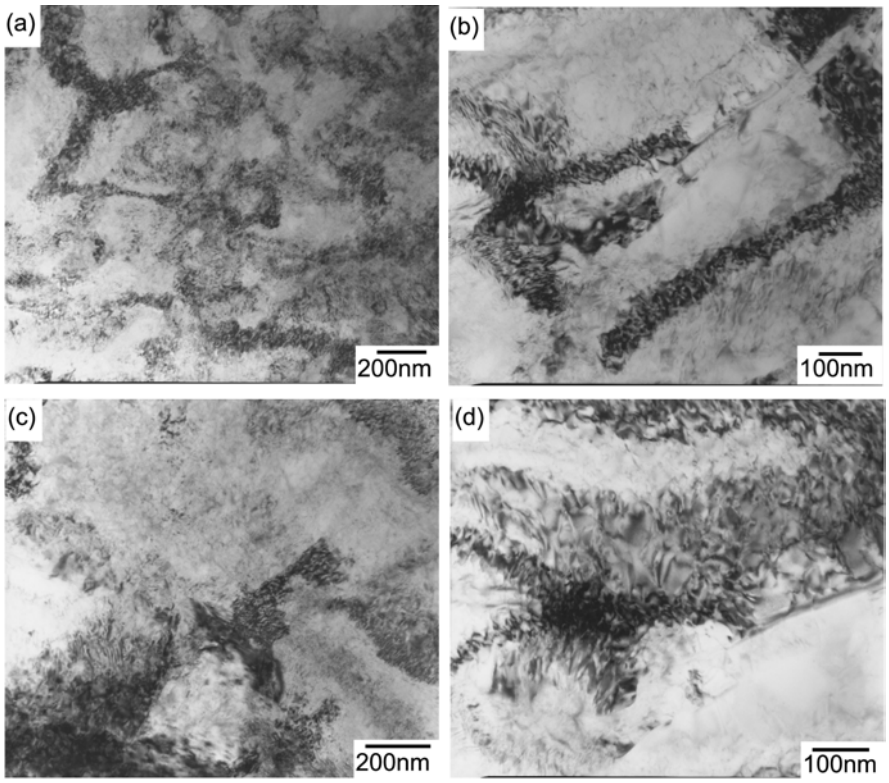

Fig. 42 TEM micrographs of compact produced by ECAE with 262 MPa of back-pressure at 300ºC

A comparison study of deformation mechanisms was performed by TEM observation of compacts produced by ECAE at 300 ºC with 262 MPa of back-pressure, Fig. 42. The microstructure comprised a high dislocation density and lattice distortion while no twins were detected compare those produced at 400 ºC. The role of twinning as a shear accommodation mechanism can explain a decrease of Vickers Hardness, Fig.43.

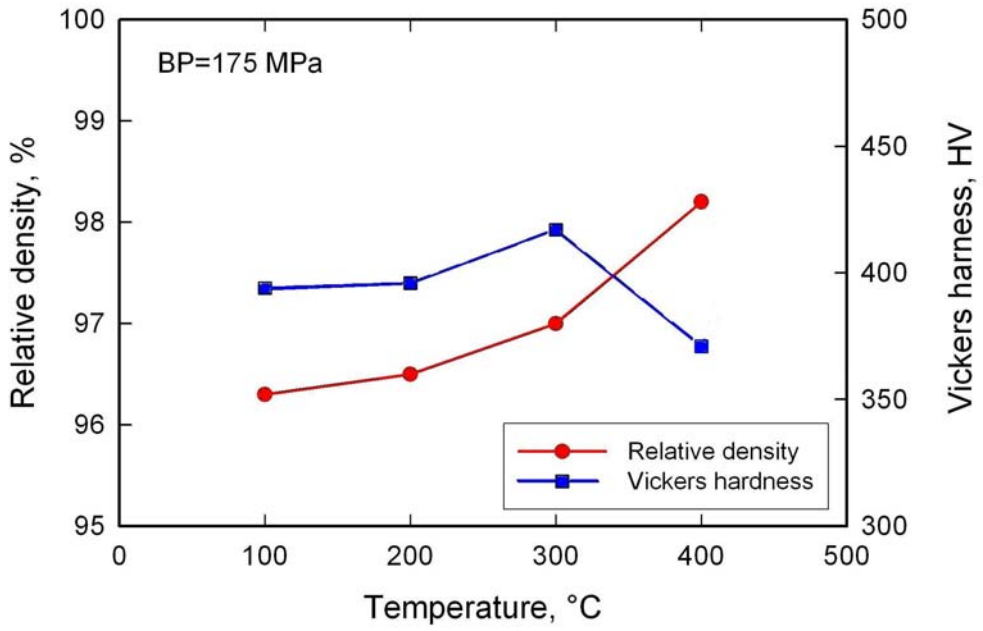

Fig. 43 Relative density and Vickers hardness as a function of temperature.

6.9 Role of Prior Heat Treatment of Powder in ECAE Compaction

As plastic shear deformation plays an important role in improving powder compaction, it is expected that a change of the alpha-to-beta phase ratio will improve the ductility of powder with consequent increase in relative density

The α/ß ratio in Ti-6Al-4V can be changed by heat treatment. Three regimes of heat treatment were carried out:

- mill annealing (heating up to 730ºC for 4 hours and furnace cooling to 25ºC)
- mill annealing (heating up to 850ºC for 4 hours and furnace cooling to 25ºC)
- ß-annealing (heating up to 1065ºC for 0.5 hour and furnace cooling to 25ºC)

.

SEM images of Ti-6Al-4V powder microstructure in as-received conditions are shown in Fig. 44a. The ß-phase fraction of 5.5% was calculated using image analysis technique. The first heat treatment produced a microstructure of discontinuous lamellar ß-phase in α-matrix, Fig. 44b. The ß-phase fraction increased to 7.5%. The

second and third heat treatment increased ß-phase fraction further to 9.3% and 10%, respectively (Fig. 44 c, d).

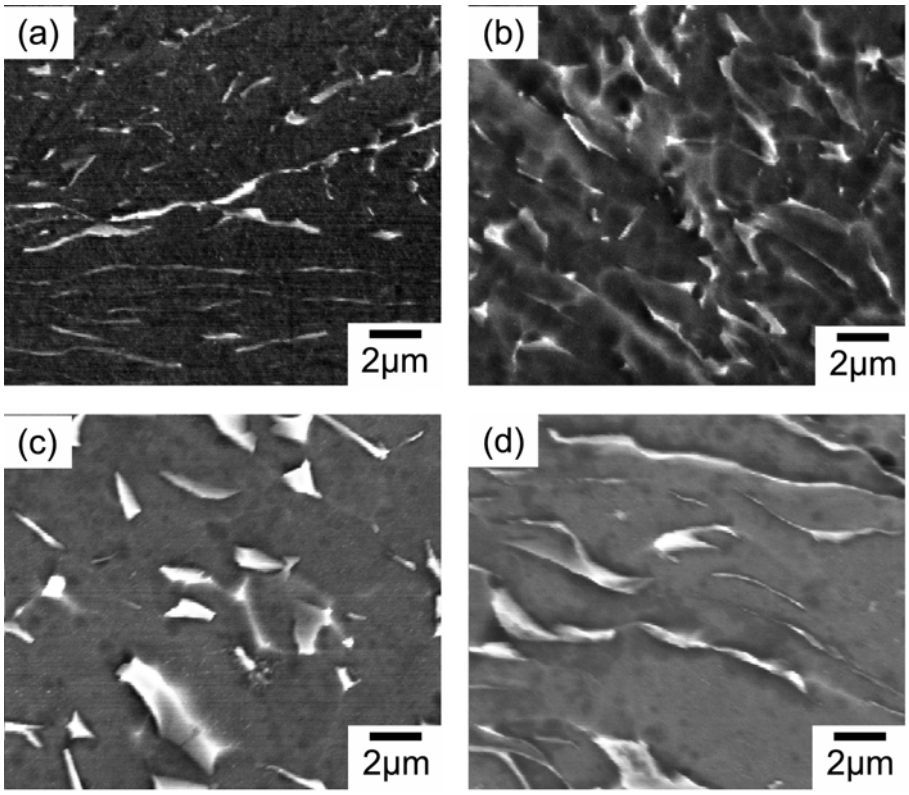

Fig. 44 SEM micrographs of powder heat treated with various conditions (a) - as-received; (b) - 730ºC, 4h; (c) - 850ºC, 4h; (d) - 1065ºC, 0.5h.

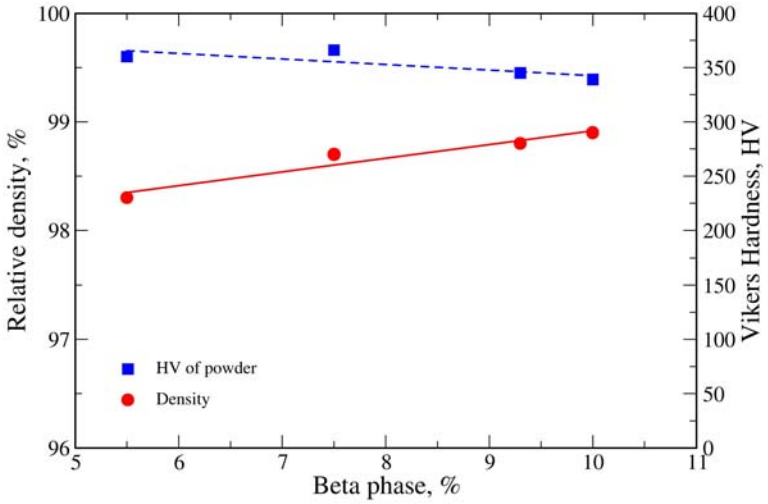

Fig. 45 Relative density and Vickers hardness of compacts produced by ECAE at 400 ºC with 350 MPa of back pressure as a function of ß - phase fraction.

The heat treated powder was further processed by ECAE at 400°C with 350 MPa back pressure in order to investigate the powder compaction capability. The results are summarized in Fig. 45. As it was expected, increasing the temperature of the heat treatments induces an increase of ß - phase fraction from 5.5% to 10%. The increased amount of more ductile ß – phase results in linear increase of relative density from 98.3% to 98.9%, Fig. 45. Vickers Hardness has linearly decreasing with increasing ß - phase but at a slower rate.

7 CONCLUSIONS

It has been shown that the use of ECAE with imposed hydrostatic pressure permits a reduction in the range of compaction temperatures required for consolidation of Ti-6Al-4V powder compared to those used in conventional practice. The temperatures are below those normally dangerous for gas contamination.

The ECAE compaction of Ti-6Al-4V powder at room temperature with a back-pressure of 262 MPa produced a billet with the relative density of 95.6% but low green strength. With temperature increase up to 400 ºC the relative density increased to 98.3% for the same processing conditions and the green strength increasing to about 750 MPa. The increase in green strength was explained by enhancement of self-diffusion obtained by creating additional diffusion paths (defects during severe shear deformation) and imposed hydrostatic pressure (back-pressure). It was shown that further increase in relative density can be obtained by increasing hydrostatic pressure component or by increase of the ß – phase fraction.

The relative density of compacts produced by ECAE at temperature of 400 ºC increases from 96.8 to 98.3 % with back pressure rising from 20 to 350 MPa, whereas Vickers Hardness increases from 360 to 412 HV. The increase in back-pressure to 480 MPa leads to an increase in relative density to 98.6%. It was shown that further increase in relative density can be obtained by increasing the hydrostatic pressure component.

The shear deformation was found to be the key-factor in improved compaction. Comparison of conventionally compacted billets with compacts produced by ECAP at the same levels of hydrostatic pressure shows an improvement of relative density by at least 2% due to shear deformation. The roles of twinning and lattice distortion in the improvement of densification have been revealed.

The application of a second ECAE pass and a holding time (1 hour) at the pre-set temperature and pressure have been studied. In both cases the improvement of the relative density was minimal to justify the additional steps technologically. The improvement of relative density by 0.4% has been observed after 4 hours sintering in vacuum furnace at 1100ºC.

It was shown that plastic deformation is an important factor for Improvement of densification. Heat treatments, such as ß – annealing, which changes the ß/α – phase ratio, leads to the further improvement of densification. It was shown that a change of ß – phase fraction from 5.5% (as-received conditions) to 10% (after heat treatment) leads to an increase in relative density from 98.3% to 98.9%.

8. SUGGESTIONS FOR FUTURE WORK

The experimental program completed indicates potential for further significant improvement in relative densities (>98.6%) and green strengths (>750MPa) with increases in applied back-pressure (>400 MPa). However, this would require an improvement to the existing die design to accommodate the increased axial loading on the forward punch. The current equipment has a forward loading limit of 27 tons. An increase in the equipment capacity would also permit the processing of billets that are larger in cross-section and length, and thus the creation of samples that would be required for full-scale property evaluation, including mechanical testing.

The current project was limited to one specific type of pre-alloyed powder. However, it is known that the morphology, composition and structure of the powder can have significant effects on the the potential for direct powder consolidation, the behaviour of the powder during consolidation and on the properties of the compact. It is thus desirable that the evaluation be extended to Ti-6Al-4V powders of different forms and consolidation potential, in order to assess the role of powder variables in determining the optimum consolidation conditions and desirable properties in the resultant consolidated product. Consideration should also be given to the selection of the alloy for consolidation and the potential for the design of novel alloy compositions that are optimised for this direct powder processing route.

The present work has produced preliminary evidence that powder microstructure may be a significant factor in determining processability. Future work should investigate the role of microstructural factors in determining the potential for consolidation, including, for example, the effects that a change in the phase ratio in the powder prior to compaction may have on relative density and green strength. The role of post-consolidation heat treatment on the integrity and properties of the processed billet should also be explored systematically.

Further work is required to improve understanding of the mechanism(s) of consolidation during direct powder consolidation at such low processing temperatures. If, as suggested, consolidation is associated with enhanced mass transport that is attributable to the severe shear deformation, mechanical alloying routes might be investigated and designed for production of solid billet from blended elemental (BE) powders, with the aim of eliminating the major shortcoming of this method, namely the non-uniformity in structure and properties.

The upper temperature limit for processing of 400ºC imposed in the present work to minimise gaseous contamination was somewhat arbitrarily defined and might be defined more precisely with appropriate experimentation. It is clear that there would be advantages to raising this limit, even modestly. Furthermore, the processing

window for different alloys might be explored to advantage to maximise the relative densities and green strengths obtainable.

The present work constitutes, in essence, a feasibility study and, while additional work is necessary to full demonstrate the potential of the approach, attention should also be given to approaches for scale-up of the process. The potential for development of technology for continuous compacting of powder based on severe shear deformation with imposed hydrostatic pressure should be evaluated.

9. REFERENCES

1. Jim Williams, Thermo-mechanical processing of high-performance Ti alloys: recent progress and future needs, J. of Materials Processing Technology, 117 (2001), 370-373.
2. Matthew J. Donachie, Jr., Titanium. A Technical Guide, Second Edition, ASM International, 2000.
3. C.A. Kelto, B.A. Kosmal, D. Eylon, F.H. Froes, Titanium powder metallurgy – A perspective, In Proceeding of Symposium “Powder Metallurgy of Titanium Alloys”, 1980, The Metallurgical Society of AIME, 1 - 19.
4. M. Hagiwara, S.J. Kim, S. Emura, Blended elemental P/M synthesis of Ti-6Al-1.7Fe-0.1Si alloy with improved high cycle fatigue strength, Scripta Materialia, **39:9** (1998), 1185 - 1190.
5. P.J. Andersen, P.C. Eloff, Development of higher performance blended elemental powder metallurgy Titanium alloys, In Proceeding of Symposium “Powder Metallurgy of Titanium Alloys”, 1980, The Metallurgical Society of AIME, 175 - 187.
6. O.M. Ivasishin, D.G. Savvakin, F. Froes, V. C. Mokson and K.A. Bondareva, Synthesis of Alloy Ti — 6Al — 4V with Low Residual Porosity by a Powder Metallurgy Method, Powder Metallurgy and Metal Ceramics **41** (2002), 382–390.
7. O.M. Ivasishin, Cost-effective manufacturing of Titanium parts with powder metallurgy approach, Presentation at ICAMP-3, November 2004, Melbourne, Australia.
8. O.M. Ivasishin, V.M. Anokhin, A.N. Demidik and D.G. Savvakin, Cost-effective blended elemental powder metallurgy of Titanium alloys for transportation applications, Key Engineering Materials **188** (2000), 55–62.
9. R.R. Boyer, J.E. Magnuson, J.W. Tripp, Characterisation of pressed and sintered Ti-6Al-4V powders, Proceeding of the AIME Symposium on Titanium Powder Metallurgy, February 1980, Las Vegas., 203-216.
10. Y. Mahajan, D. Eylon, R. Bacon, F.H. Froes, Microstructure property correlation in cold pressed and sintered elemental Ti-6Al-4V powder compact, Proceeding of the AIME Symposium on Titanium Powder Metallurgy, February 1980, Las Vegas.
11. P.J. Andersen, P.C. Eloff, Development of higher performance blended elemental powder metallurgu Ti alloys, Proceeding of the AIME Symposium on Titanium Powder Metallurgy, February 1980, Las Vegas.
12. D.P. Delo, H.R. Piehler, Early stage consolidation mechanisms during hot isostatic pressing of Ti-6Al-4V powder compacts, Acta Materialia, **47:9** (1999), 2841–2852.

13. T. C. Lowe, R. Z. Valiev, Producing nanoscale microstructures through severe plastic deformation, JOM. April (2000), pp. 27.
14. R. Lapovok, The role of Back-Pressure in Equal Channel Angular Extrusion, Journal of Materials Science, **40:2**, (2005), 341-346.
15. J. Robertson, J.-T. Im, I. Karaman, K.T. Hartwig, I.E. Anderson, Cosolidation of aamorphous copper based powder by equal channel angular extrusion, Journal of Non-crystalline Solids **317** (2003), 144-151.
16. R. Lapovok, P.F. Thomson, Densification of Magnesium Particles by ECAP with a Back-Pressure, NANOSPD, Proceedings of the 2nd International Conference on Nanomaterials by Severe Plastic Deformation: Fundamentals - Processing - Applications, Dec. 9-13, 2003, Vienna, Austria, (2003), 551-557.
17. Kaculi, T. Xhemal, M.N. Srinivasan, K.T. Hartwig, Use of mechanical alloying and equal channel angular extrusion to produce nanostructured titanium silicide, In Proceeding of the Conference "Processing and Fabrication of Advanced Materials XII", Oct. 13-15, 2003, ASM International, 315-329.
18. Bhosle, E.G. Baburaj, M.Miranova, K. Salama, Materials, Dehydrogenation of TiH_2, Materials Science & Engineering **A356** (2003) 190–199.
19. R.E. Goforth N.D. Frey S.L. Semiatin, V.M. Segal and D.P. DeLo, Workability of Commercial-Purity Titanium and 4340 Steel During Equal Channel Angular Extrusion at Cold-Working Temperatures, Met and Mat Trans. A **30A** (1999) 1425–1435.
20. P.W.J. McKenzie, R. Lapovok, Y. Estrin Influence of Back Pressure on ECAP Processed AA 6016: Modeling and Experiment, Acta Materialia, Vol **55/2** (2007), pp 2985-2993.
21. Lapovok R., Damage Evolution under Severe Plastic Deformation, International Journal of Fracture, **115: 2** (2002), 159-172.
22. Guney Guven Yapici, Ibtahim Krraman, Zhi-Ping Luo, Mechanical Twinning and Texture Evolution in Severly Deformed Ti-6Al-4V at High Temperatures Acta mater. **54** (2006), 3755–3771.